Interpretation of ATLAS and CMS Higgs measurements in STXS and EFT

Nikita Belyaev

on Behalf of the ATLAS and CMS Collaborations

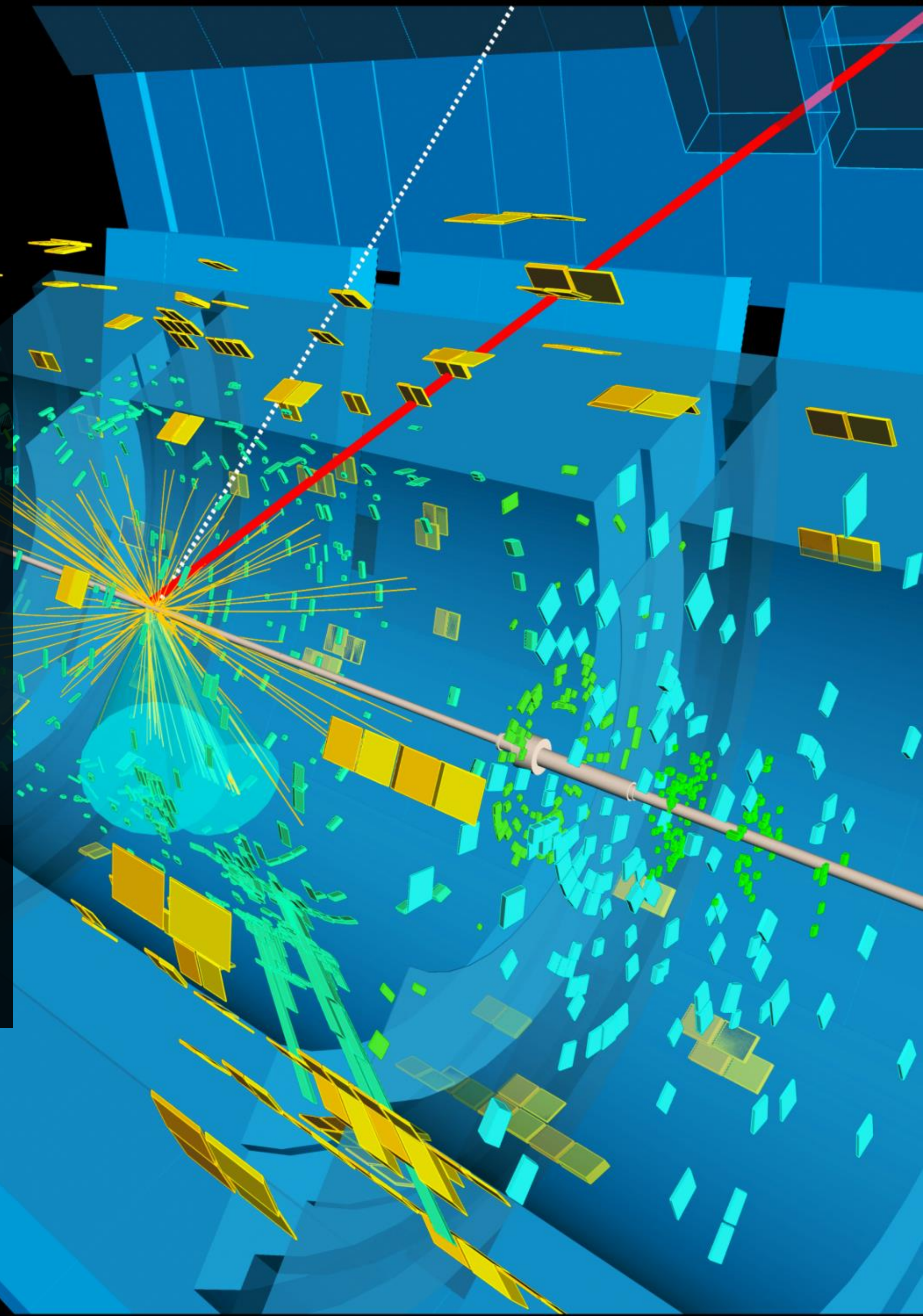

MEPhI

Introduction: STXS

- The Simplified Template Cross-Section (STXS) measurements, which are the most common type of the results in ATLAS and CMS, are often used to probe the Higgs boson couplings.
- The advantage of STXS measurements are the following:
  - ➕ Maximizing experimental sensitivity
  - ➕ Isolation of possible BSM effects
  - ➖ Not fully fiducial
  - ➕ Minimizing the theoretical uncertainties
  - ➕ Suitable for global combinations
  - ➖ No Higgs decay information

Introduction: STXS

- The Simplified Template Cross-Section (STXS) measurements, which are the most common type of the results in ATLAS and CMS, are often used to probe the Higgs boson couplings.
- The advantage of STXS measurements are the following:
  - \+ Maximizing experimental sensitivity
  - \+ Isolation of possible BSM effects
  - − Not fully fiducial
  - \+ Minimizing the theoretical uncertainties
  - \+ Suitable for global combinations
  - − No Higgs decay information
- The STXS measurements are performed in two steps:
  - The Stage 0 bin definitions essentially correspond to the production mode measurements.

$\boxed{gg \to H}$

$\boxed{\text{EW } qqH} = \text{VBF} + V(\to qq)H$

LHCHXSWG-2019-003

Introduction: STXS

- The Simplified Template Cross-Section (STXS) measurements, which are the most common type of the results in ATLAS and CMS, are often used to probe the Higgs boson couplings.
- The advantage of STXS measurements are the following:
  - ✚ Maximizing experimental sensitivity
  - ✚ Isolation of possible BSM effects
  - ▬ Not fully fiducial
  - ✚ Minimizing the theoretical uncertainties
  - ✚ Suitable for global combinations
  - ▬ No Higgs decay information
- The STXS measurements are performed in two steps:
  - The Stage 0 bin definitions essentially correspond to the production mode measurements.
  - The Stage 1 brings additional bins based on kinematics.

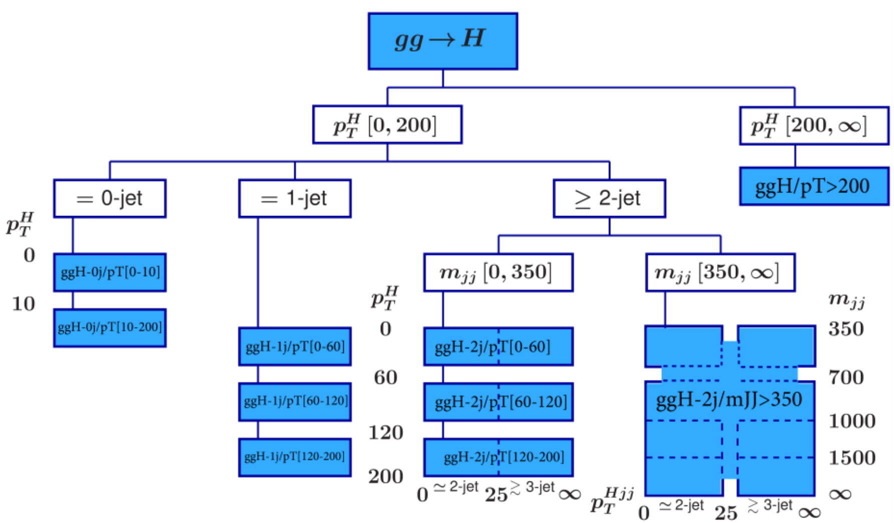

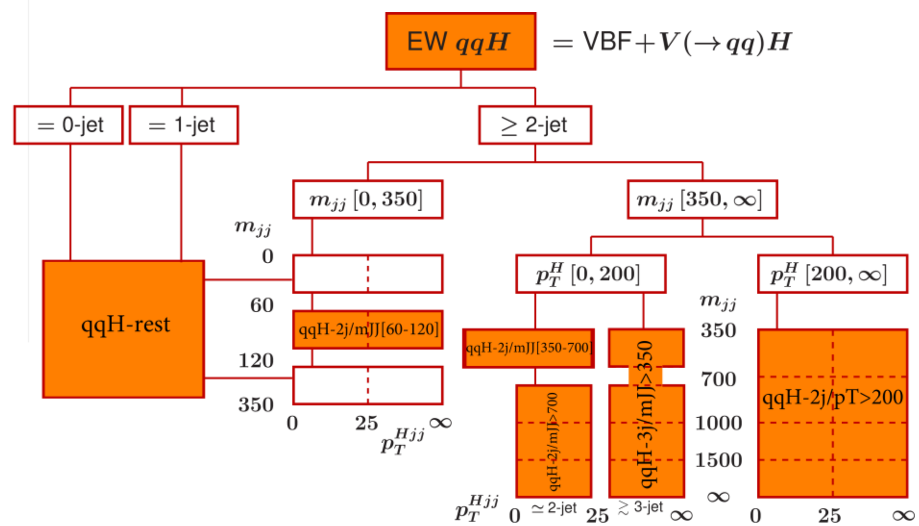

LHCHXSWG-2019-003

Introduction: STXS

- The Simplified Template Cross-Section (STXS) measurements, which are the most common type of the results in ATLAS and CMS, are often used to probe the Higgs boson couplings.
- The advantage of STXS measurements are the following:
  - ✚ Maximizing experimental sensitivity
  - ✚ Isolation of possible BSM effects
  - ▬ Not fully fiducial
  - ✚ Minimizing the theoretical uncertainties
  - ✚ Suitable for global combinations
  - ▬ No Higgs decay information
- The STXS measurements are performed in two steps:
  - The Stage 0 bin definitions essentially correspond to the production mode measurements.
  - The Stage 1 brings additional bins based on kinematics.

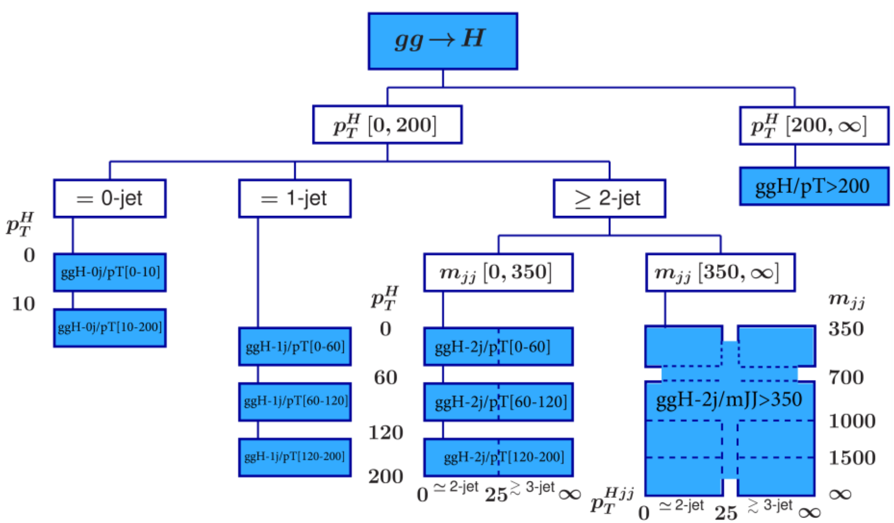

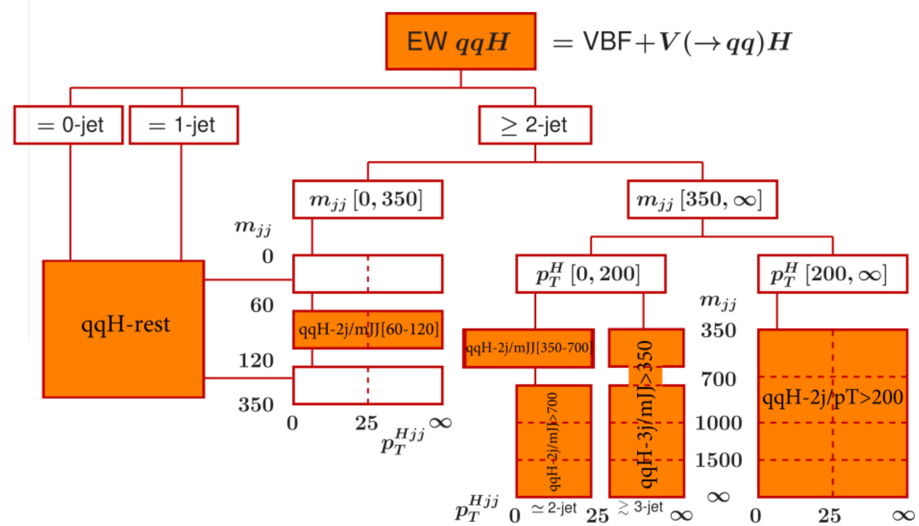

- The goal is that the full granularity should become accessible in the combination of all decay channels.

LHCHXSWG-2019-003

STXS measurements: an example

- The 4l CMS STXS measurements with the full Run II dataset are done in 7 Stage 0 and 22 Stage 1 bins.
- Expected fraction of signal events is estimated per production mode in the different categories.
- Cross sections in each bin are extracted from the fits in categories.

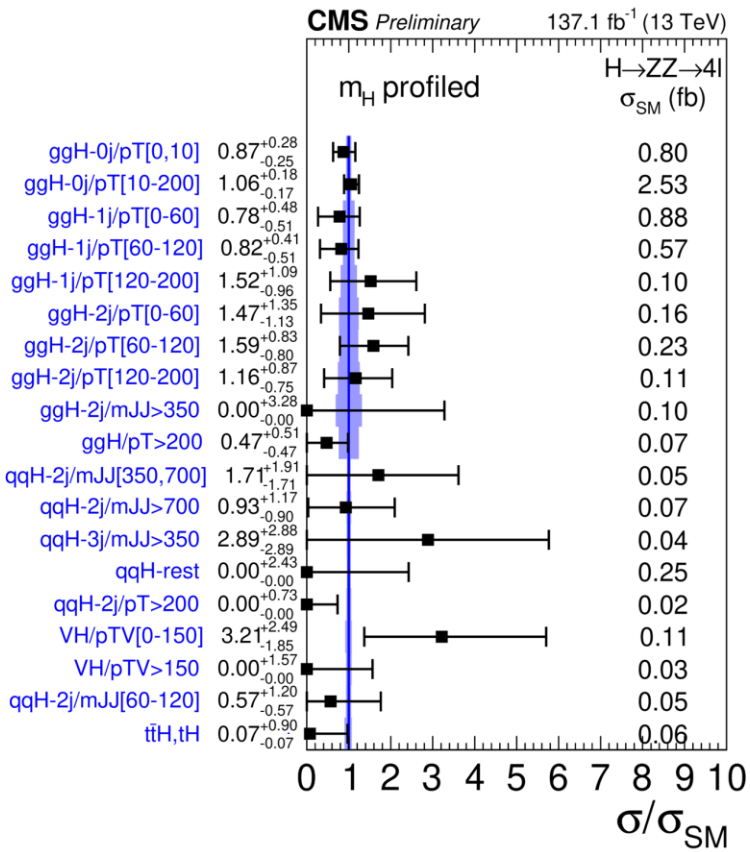

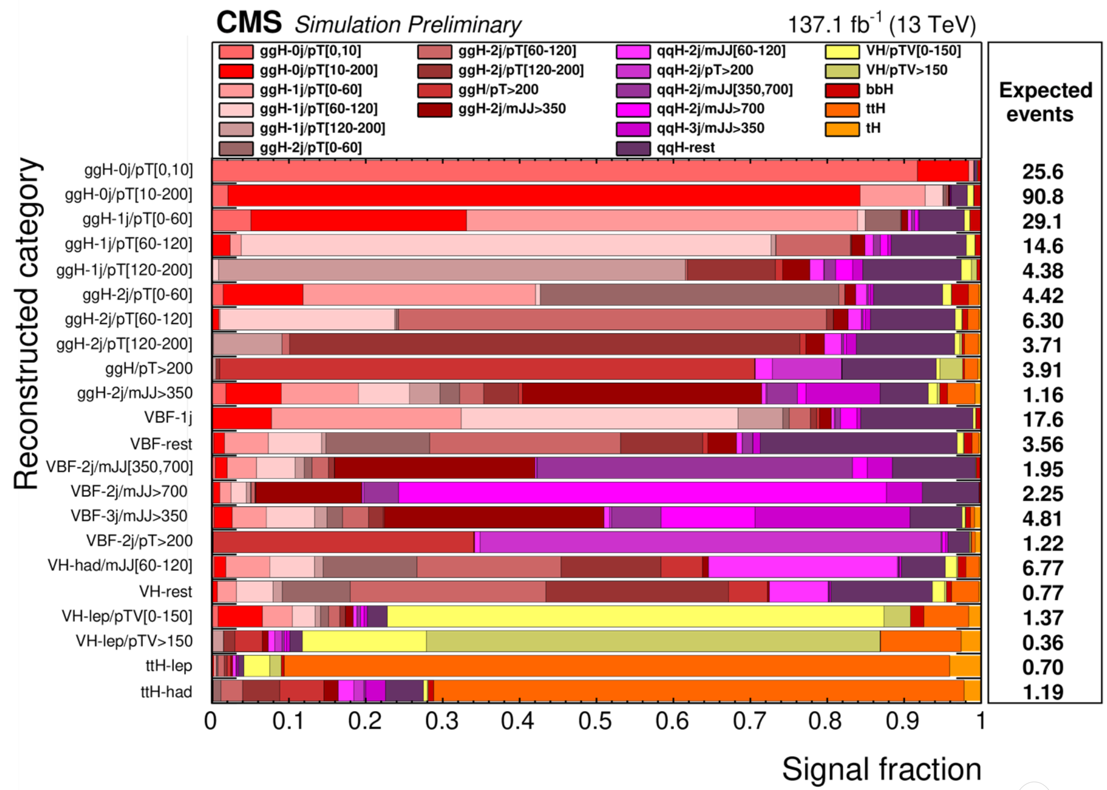

- More details about the STXS measurements for presented EFT results can be found at W. Leight and S. Jiggins talks (ZZ/WW and $bb/\tau\tau$ modes, respectively).

Effective field theory approach

- After Run 1 discovery of the Higgs boson, the increased number of Higgs decays allows improved precision in the couplings and cross section measurements to test the compatibility of the SM predictions and search for possible deviations.
- One of the most promising tools in this field is the Effective Field Theory (EFT) approach, in which the SM Lagrangian is supplemented by new operators with canonical dimensions D larger than 4:

$$\mathcal{L}_{\rm eff} = \mathcal{L}_{\rm SM} + \sum_i \frac{c_i^{(5)}}{\Lambda}\mathcal{O}_i^{(5)} + \sum_i \frac{c_i^{(6)}}{\Lambda^2}\mathcal{O}_i^{(6)} + \sum_i \frac{c_i^{(7)}}{\Lambda^3}\mathcal{O}_i^{(7)} + \sum_i \frac{c_i^{(8)}}{\Lambda^4}\mathcal{O}_i^{(8)} + \cdots$$

where c_i are so-called Wilson coefficients and $\mathcal{O}_i^{(D)}$ are the operators of dimension D.

- This framework can be used to interpret the STXS results (but also applicable for the interpretation of differential cross sections and kinematic measurements):
  - ➢ The Higgs boson production cross-section in STXS region p can be expressed as:

$$\sigma_p = \sigma_{p,\mathrm{SM}} + \sigma_{p,\mathrm{int}} + \sigma_{p,\mathrm{BSM}}$$

  - ➢ Its ratio to the SM can be then parameterized as follows:

$$\frac{\sigma_p}{\sigma_{p,\mathrm{SM}}} = 1 + \sum_i A_i^{\sigma_p} c_i + \sum_{ij} B_{ij}^{\sigma_p} c_i c_j$$

  where $A_i^{\sigma_p}$ and $B_{ij}^{\sigma_p}$ are coefficients independent of the c_i and determined from simulation.

- Main simulation tool: *SMEFTsim* model for the *MadGraph5_aMC@NLO* Monte Carlo generator.

ATL-PHYS-PUB-2019-042

EFT bases

- A complete and non-redundant set of higher-dimensional operators forms so-called EFT basis.
- For each specific type of interaction, EFT bases can be constructed in several different ways, but all of them are equivalent in terms of physics effects.
- For example, CP-violating operators of the Higgs Effective Lagrangian (HEL) model in the gauge eigenbasis can be written as:

$$\mathcal{L}_{CP} = \frac{ig\ \tilde{c}_{HW}}{m_W^2} D^\mu \Phi^\dagger T_{2k} D^\nu \Phi \widetilde{W}^k_{\mu\nu} + \frac{ig'\ \tilde{c}_{HB}}{m_W^2} D^\mu \Phi^\dagger D^\nu \Phi \widetilde{B}_{\mu\nu} + \frac{g'^2\ \tilde{c}_\gamma}{m_W^2} \Phi^\dagger \Phi B_{\mu\nu} \widetilde{B}^{\mu\nu}$$
$$+ \frac{g_s^2\ \tilde{c}_g}{m_W^2} \Phi^\dagger \Phi G^a_{\mu\nu} \widetilde{G}^{\mu\nu}_a + \frac{g^3\ \tilde{c}_{3W}}{m_W^2} \epsilon_{ijk} W^i_{\mu\nu} W^{\nu j}{}_\rho \widetilde{W}^{\rho\mu k} + \frac{g_s^3\ \tilde{c}_{3G}}{m_W^2} f_{abc} G^a_{\mu\nu} G^{\nu b}{}_\rho \widetilde{G}^{\rho\mu c}$$

- There a many different bases describing the BSM Higgs boson interactions: Warsaw (SMEFT) basis, SILH basis, Higgs basis and others.
- But sometimes it is reasonable to work only with a small subset of new operators, not with the whole basis.
  - Example: an effective amplitude of the HVV interaction can be written as follows:

$$A(\mathrm{HVV}) \sim \left[a_1^{\mathrm{VV}} + \frac{\kappa_1^{\mathrm{VV}} q_1^2 + \kappa_2^{\mathrm{VV}} q_2^2}{\left(\Lambda_1^{\mathrm{VV}}\right)^2} \right] m_{\mathrm{V}1}^2 \epsilon_{\mathrm{V}1}^* \epsilon_{\mathrm{V}2}^* + a_2^{\mathrm{VV}} f_{\mu\nu}^{*(1)} f^{*(2)\mu\nu} + a_3^{\mathrm{VV}} f_{\mu\nu}^{*(1)} \tilde{f}^{*(2)\mu\nu}$$

EFT measurements in the bb channel (ATLAS)

- The STXS measurements and their EFT interpretation were done with the $H \to bb$ decay channel for the W/ZH production.
- Cross-sections are measured as a function of the gauge boson transverse momentum in kinematic fiducial volumes.
- One-dimensional limits on four linear combinations of the Wilson coefficients in the SILH basis have been set.

Coefficient	Operator
$\bar{c}_{HW}$	$i\,(D^\mu H)^\dagger\,\sigma^a\,(D^\nu H)\,W^a_{\mu\nu}$
$\bar{c}_{HB}$	$i\,(D^\mu H)^\dagger\,(D^\nu H)\,B_{\mu\nu}$
$\bar{c}_W$	$\frac{i}{2}\left(H^\dagger\sigma^a \overleftrightarrow{D}^\mu H\right) D^\nu W^a_{\mu\nu}$
$\bar{c}_B$	$\frac{i}{2}\left(H^\dagger \overleftrightarrow{D}^\mu H\right) \partial^\nu B_{\mu\nu}$
$\bar{c}_d$	$y_d\lvert H\rvert^2 \bar{Q}_\mathrm{L} H d_\mathrm{R}$

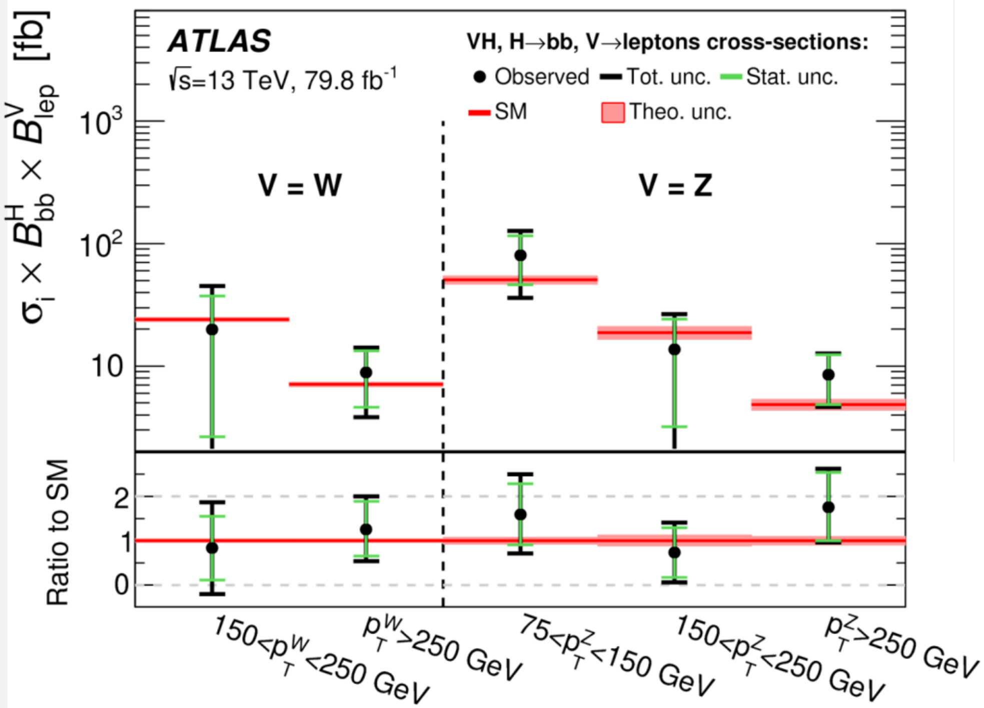

Coefficient	Expected interval	Observed interval
	Results at 68% confidence level	
$\bar{c}_{HW}$	[−0.003, 0.002]	[−0.001, 0.004]
(interference only	[−0.002, 0.003]	[−0.001, 0.005])
$\bar{c}_{HB}$	[−0.066, 0.013]	[−0.078, −0.055] ⋃ [0.005, 0.019]
(interference only	[−0.016, 0.016]	[−0.005, 0.030])
$\bar{c}_W - \bar{c}_B$	[−0.006, 0.005]	[−0.002, 0.007]
(interference only	[−0.005, 0.005]	[−0.002, 0.008])
$\bar{c}_d$	[−1.5, 0.3]	[−1.6, −0.9] ⋃ [−0.3, 0.4]
(interference only	[−0.4, 0.4]	[−0.2, 0.7])
	Results at 95% confidence level	
$\bar{c}_{HW}$	[−0.018, 0.004]	[−0.019,−0.010] ⋃ [−0.005, 0.006]
(interference only	[−0.005, 0.005]	[−0.003, 0.008])
$\bar{c}_{HB}$	[−0.078, 0.024]	[−0.090, 0.032]
(interference only	[−0.033, 0.033]	[−0.022, 0.049])
$\bar{c}_W - \bar{c}_B$	[−0.034, 0.008]	[−0.036,−0.024] ⋃ [−0.009, 0.010]
(interference only	[−0.009, 0.010]	[−0.006, 0.014])
$\bar{c}_d$	[−1.7, 0.5]	[−1.9, 0.7]
(interference only	[−0.8, 0.8]	[−0.6, 1.1])

- All measurements are found to be in agreement with the Standard Model predictions.

HIGG-2018-50

EFT measurements in the bb channel (ATLAS)

- The same measurements as in the previous analysis, but with the whole Run II dataset.
- The key improvement compared to the previous analysis is the addition of a reconstructed-event category with $p_T > 250$ GeV.
- The STXS measurements are now used to constrain the coefficients of the operators in the Warsaw basis.

Coefficient	Operator
c_{HWB}	$O_{HWB} = H^\dagger \tau^I H W^I_{\mu\nu} B^{\mu\nu}$
c_{HW}	$O_{HW} = H^\dagger H W^I_{\mu\nu} W_I^{\mu\nu}$
c_{Hq3}	$O^{(3)}_{Hq} = (H^\dagger i \overleftrightarrow{D}^I_\mu H)(\bar{q}_p \tau^I \gamma^\mu q_r)$
c_{Hu}	$O_{Hu} = (H^\dagger i \overleftrightarrow{D}_\mu H)(\bar{u}_p \gamma^\mu u_r)$
c_{dH}	$O_{dH} = (H^\dagger H)(\bar{q} d H)$

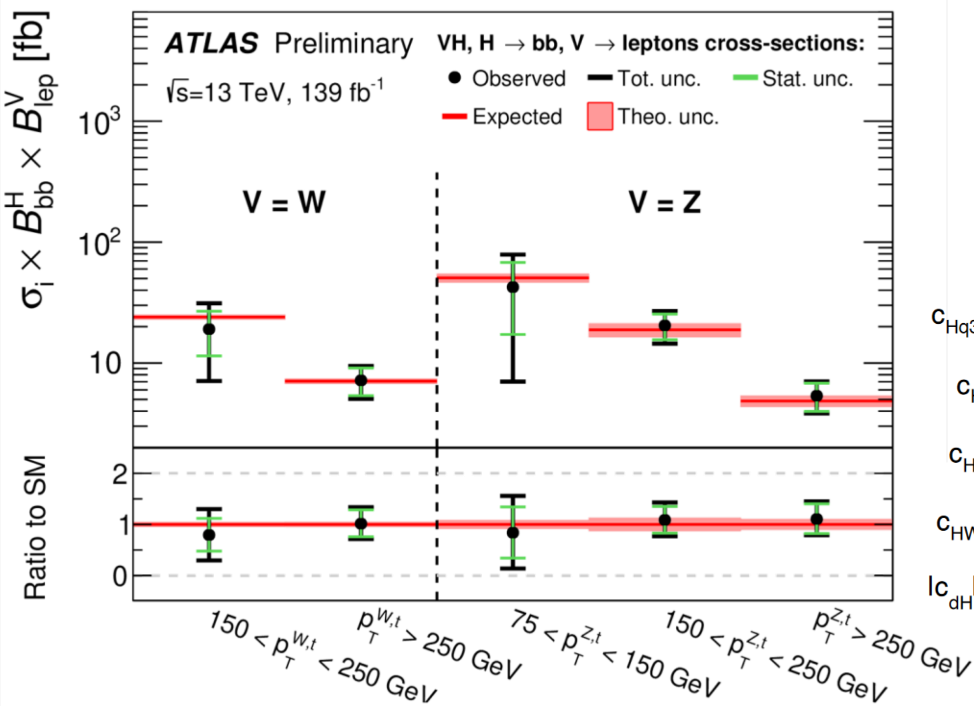

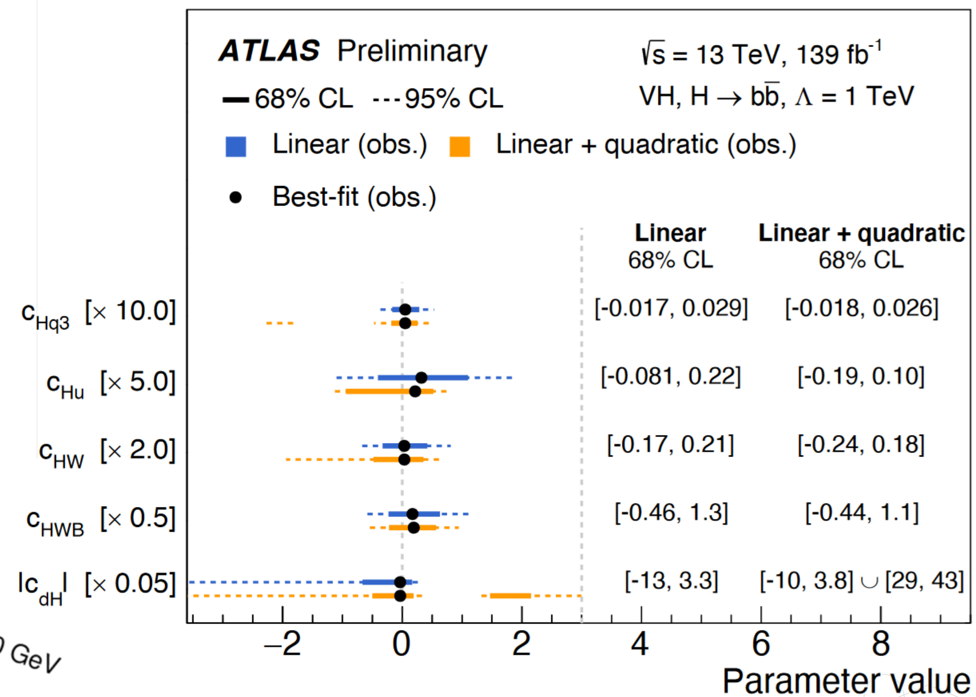

- The obtained results are all consistent with the Standard Model expectations.

The results will be published shortly (HIGG-2018-51)

More EFT measurements in the bb channel (ATLAS)

- The STXS measurements and their EFT interpretation were also done in the boosted $VH/H \to bb$ channel.
- The high-p_T measurements are particularly interesting due to their sensitivity to BSM physics.
- The STXS measurements are used to constrain the coefficients of the operators in the Warsaw basis.

Coefficient	Operator
$\lvert c_{dH} \rvert$	$(H^\dagger H)(\overline{q}_p d_r H)$
c_{HW}	$H^\dagger H W^I_{\mu\nu} W^{I\mu\nu}$
c_{HWB}	$H^\dagger \tau^I H W^I_{\mu\nu} B^{\mu\nu}$
$c^{(3)}_{Hq}$	$H^\dagger i \overleftrightarrow{D}^I_\mu H (\overline{q}_p \tau^I \gamma^\mu q_r)$
c_{Hu}	$H^\dagger i \overleftrightarrow{D}_\mu H (\overline{u}_p \gamma^\mu u_r)$

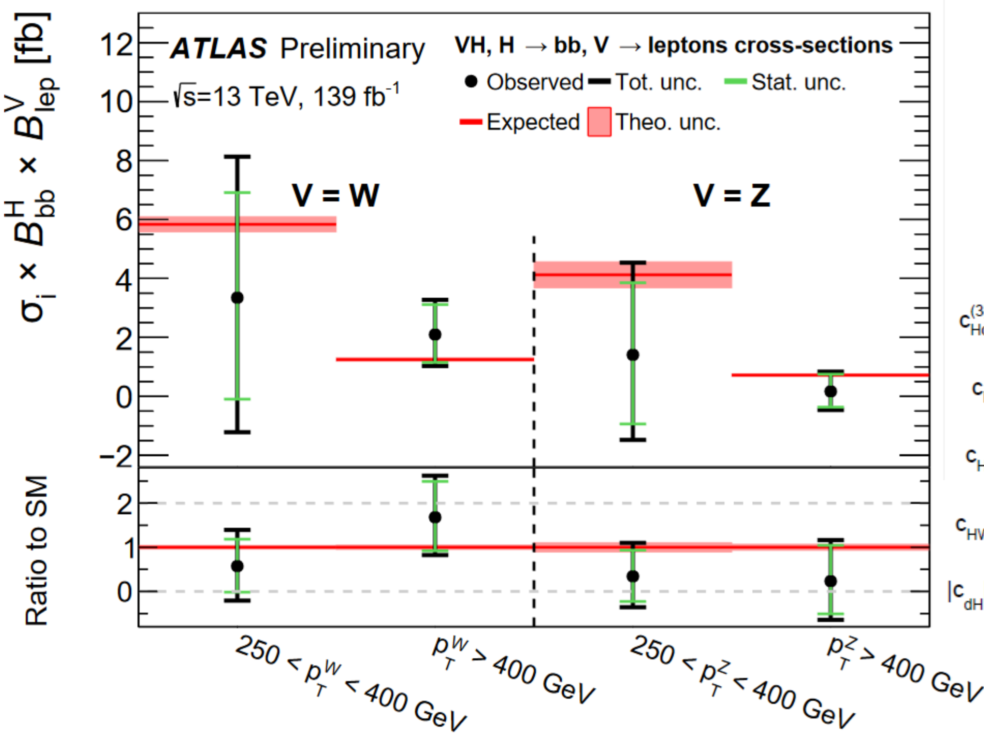

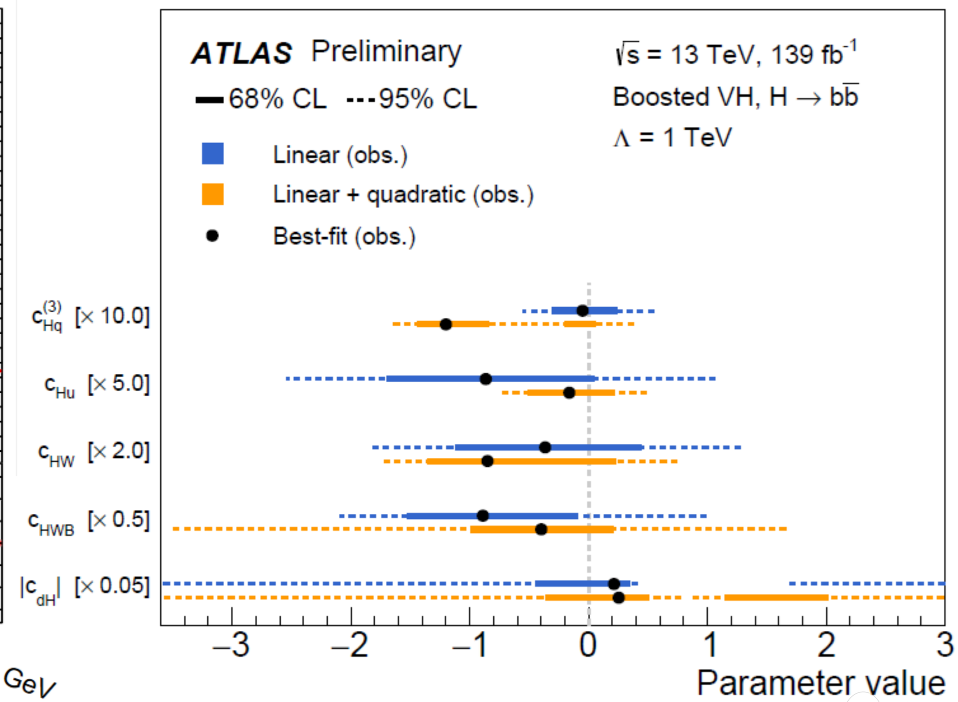

- All results are in agreement with the Standard Model predictions.

The results will be published shortly (HIGG-2018-52)

EFT measurements in the $4l$ channel (ATLAS)

- The EFT operators in the SMEFT formalism probed in this analysis:

CP-even			CP-odd			Impact on	
Operator	Structure	Coeff.	Operator	Structure	Coeff.	production	decay
O_{uH}	$HH^\dagger \bar{q}_p u_r \tilde{H}$	c_{uH}	O_{uH}	$HH^\dagger \bar{q}_p u_r \tilde{H}$	$c_{\tilde{u}H}$	ttH	-
O_{HG}	$HH^\dagger G^A_{\mu\nu} G^{\mu\nu A}$	c_{HG}	$O_{H\tilde{G}}$	$HH^\dagger \tilde{G}^A_{\mu\nu} G^{\mu\nu A}$	$c_{H\tilde{G}}$	ggF	Yes
O_{HW}	$HH^\dagger W^l_{\mu\nu} W^{\mu\nu l}$	c_{HW}	$O_{H\widetilde{W}}$	$HH^\dagger \widetilde{W}^l_{\mu\nu} W^{\mu\nu l}$	$c_{H\widetilde{W}}$	VBF, VH	Yes
O_{HB}	$HH^\dagger B_{\mu\nu} B^{\mu\nu}$	c_{HB}	$O_{H\tilde{B}}$	$HH^\dagger \tilde{B}_{\mu\nu} B^{\mu\nu}$	$c_{H\tilde{B}}$	VBF, VH	Yes
O_{HWB}	$HH^\dagger \tau^l W^l_{\mu\nu} B^{\mu\nu}$	c_{HWB}	$O_{H\widetilde{W}B}$	$HH^\dagger \tau^l \widetilde{W}^l_{\mu\nu} B^{\mu\nu}$	$c_{H\widetilde{W}B}$	VBF, VH	Yes

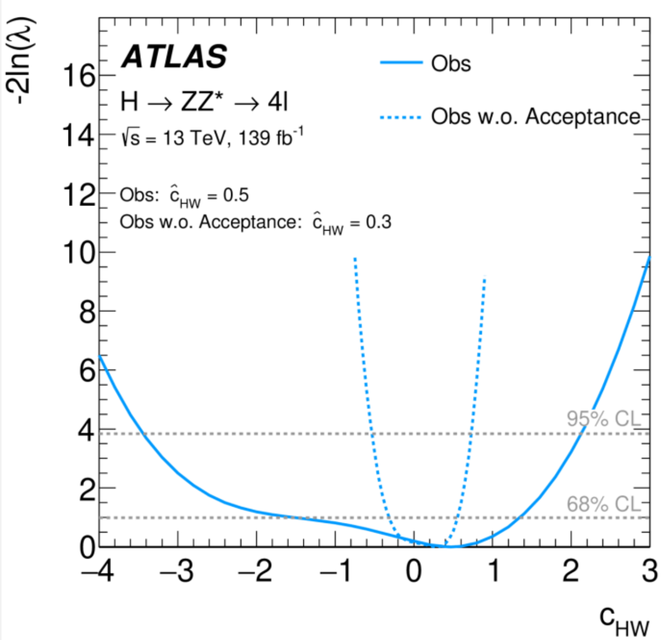

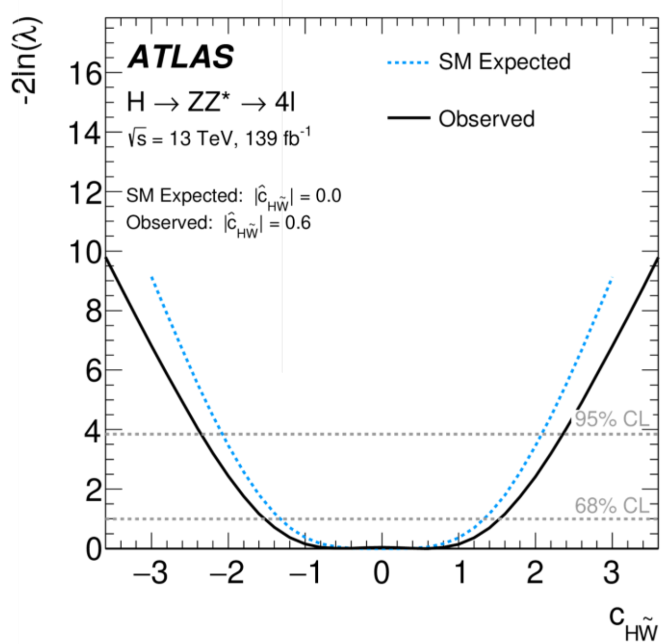

- 1D and 2D scans over the SMEFT Wilson coefficients were produced (one or two non-zero coefficients).
- Quadratic terms are taken into account in addition to the linear ones, due to their significant contribution.
- The test statistic is used to perform the measurements:

$$q(\vec{\sigma}) = -2\ln\frac{\mathcal{L}(\vec{\sigma}, \hat{\hat{\theta}}(\vec{\sigma}))}{\mathcal{L}(\hat{\vec{\sigma}}, \hat{\theta})} = -2\ln\lambda(\vec{\sigma})$$

- The acceptance correction is also considered.
- The constraints on the Wilson coefficients are obtained.

HIGG-2018-28

EFT measurements in the $4l$ channel (ATLAS)

CP-even couplings

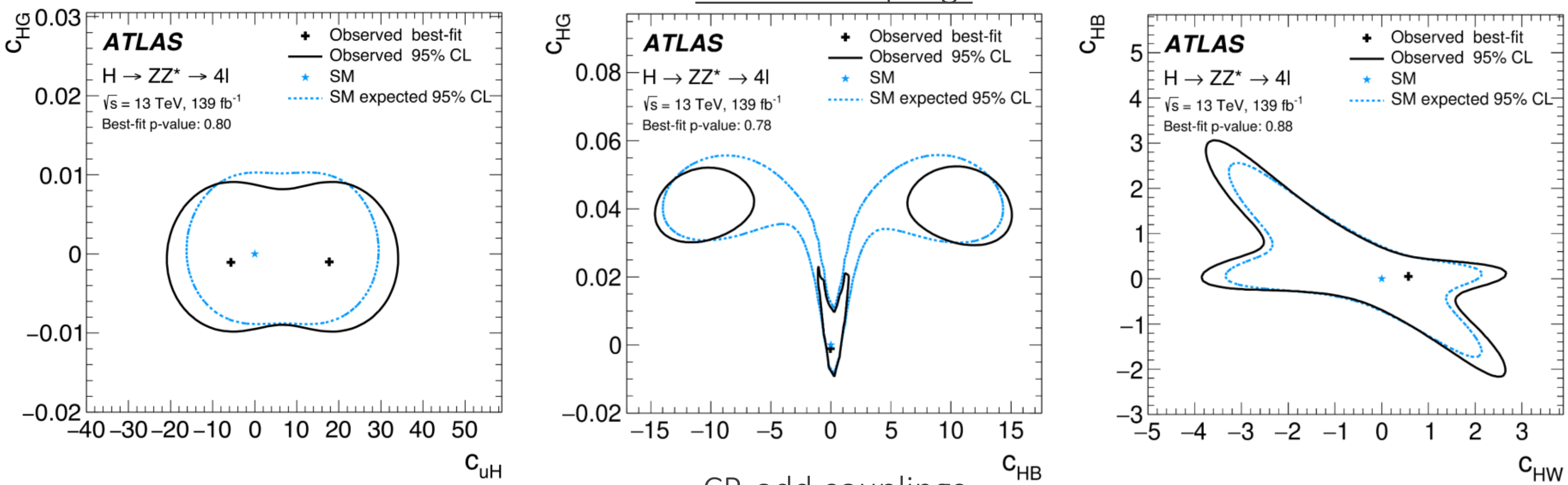

CP-odd couplings

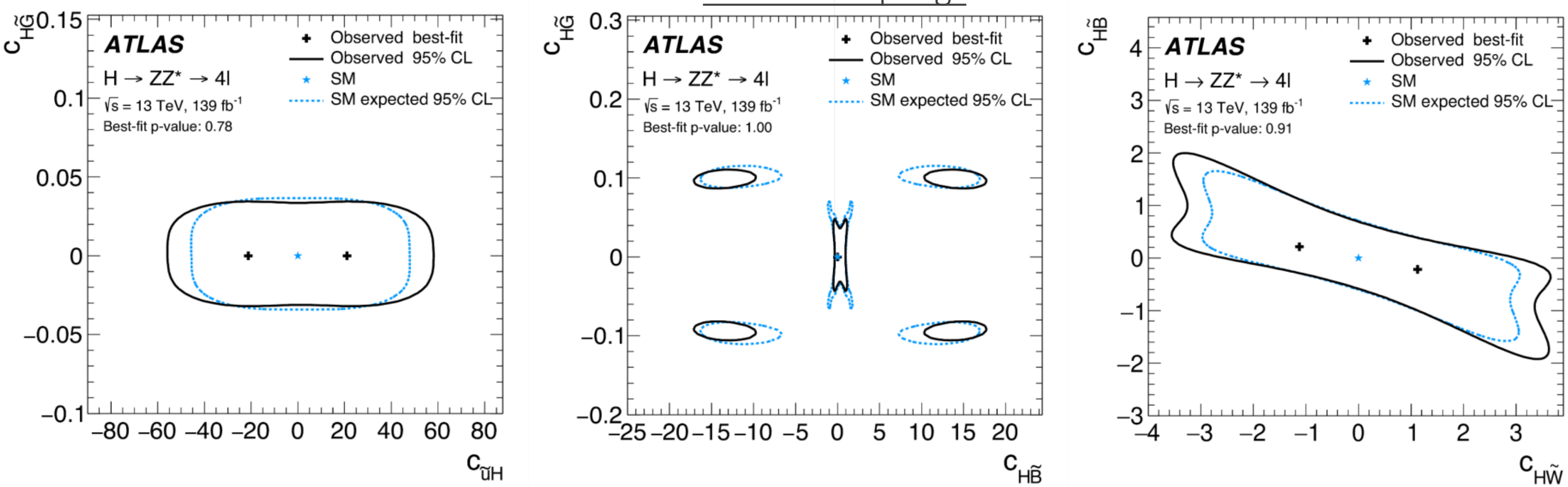

HIGG-2018-28

EFT measurements in the $4l$ channel (ATLAS)

CP-even couplings

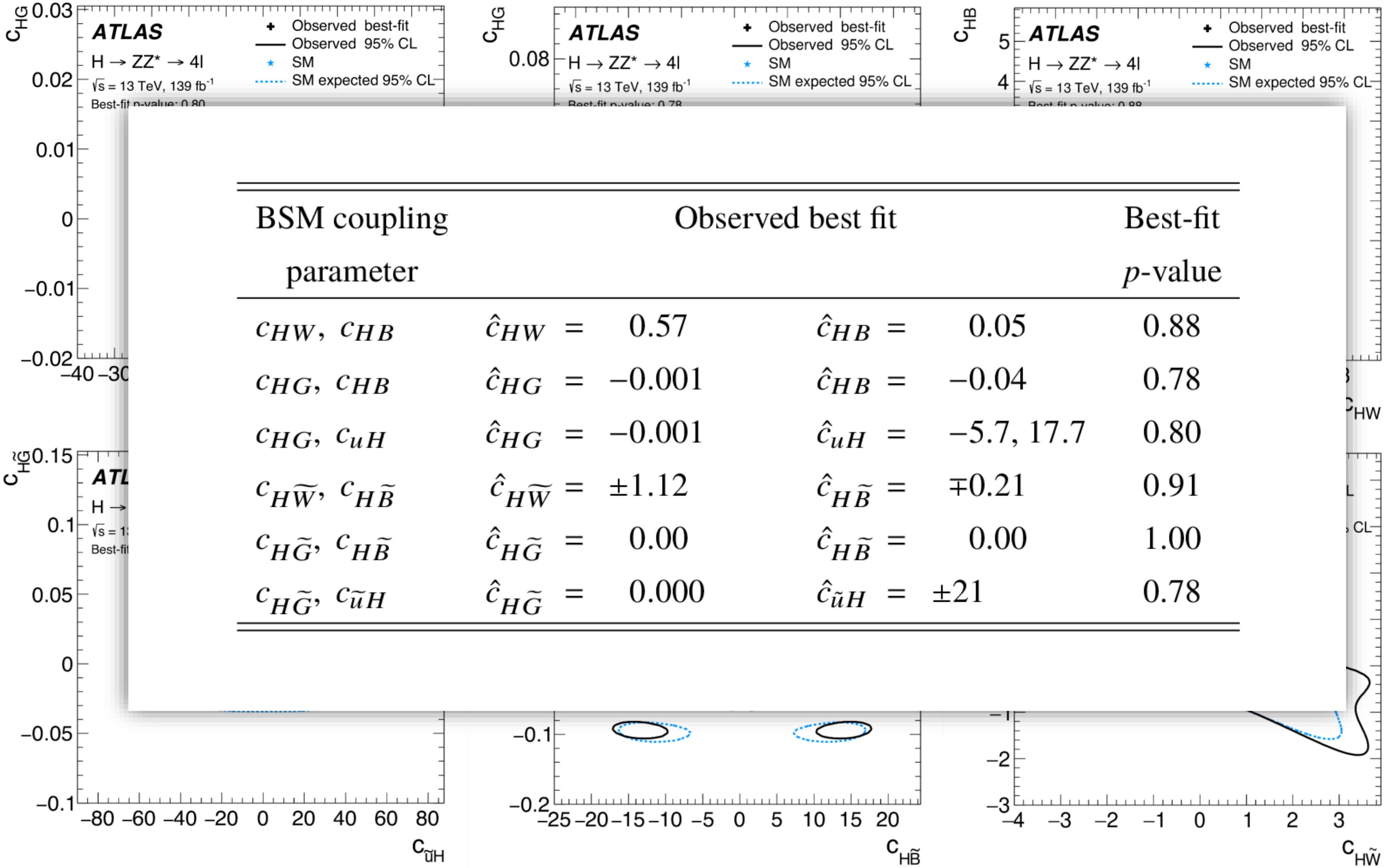

BSM coupling parameter	Observed best fit		Best-fit p-value
c_{HW}, c_{HB}	$\hat{c}_{HW} = 0.57$	$\hat{c}_{HB} = 0.05$	0.88
c_{HG}, c_{HB}	$\hat{c}_{HG} = -0.001$	$\hat{c}_{HB} = -0.04$	0.78
c_{HG}, c_{uH}	$\hat{c}_{HG} = -0.001$	$\hat{c}_{uH} = -5.7, 17.7$	0.80
$c_{H\widetilde{W}}, c_{H\widetilde{B}}$	$\hat{c}_{H\widetilde{W}} = \pm 1.12$	$\hat{c}_{H\widetilde{B}} = \mp 0.21$	0.91
$c_{H\widetilde{G}}, c_{H\widetilde{B}}$	$\hat{c}_{H\widetilde{G}} = 0.00$	$\hat{c}_{H\widetilde{B}} = 0.00$	1.00
$c_{H\widetilde{G}}, c_{\tilde{u}H}$	$\hat{c}_{H\widetilde{G}} = 0.000$	$\hat{c}_{\tilde{u}H} = \pm 21$	0.78

HIGG-2018-28

EFT measurements in the $4l$ channel (ATLAS)

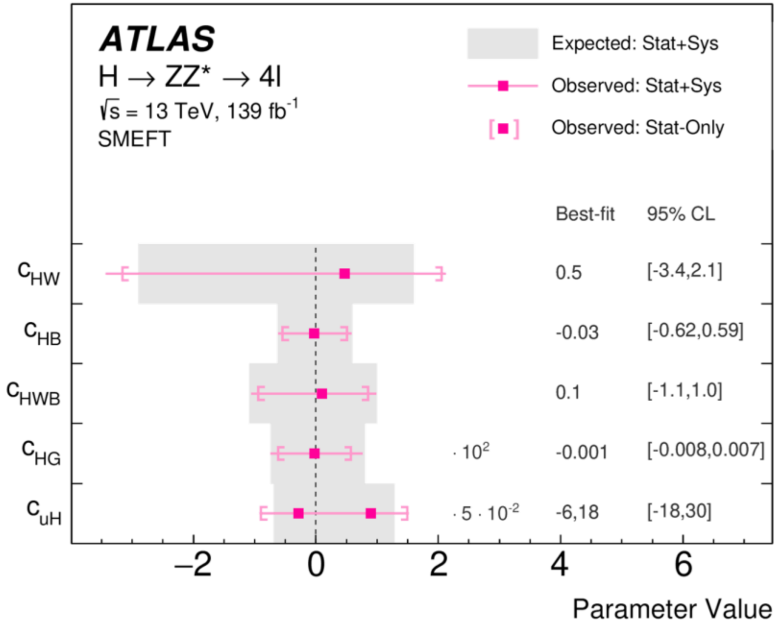

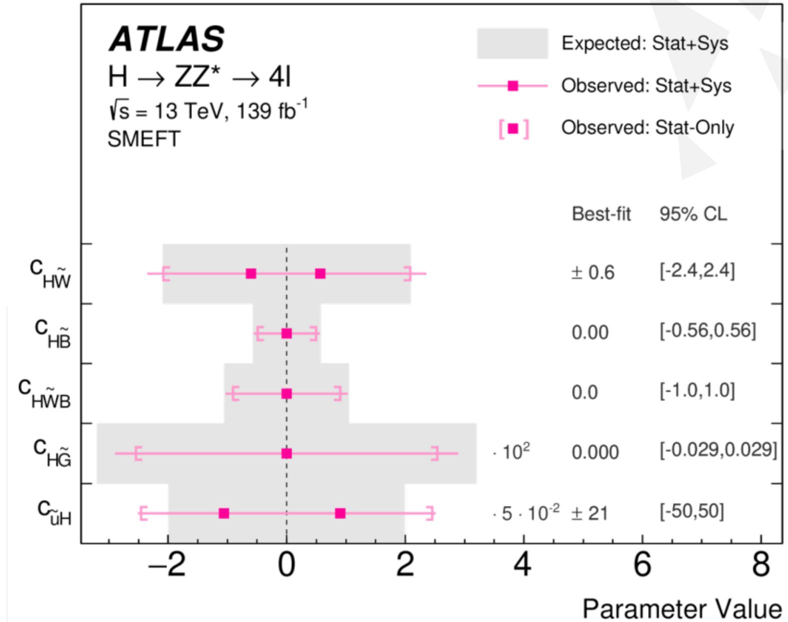

EFT coupling	Expected		Observed		Best-fit	Best-fit
parameter	68% CL	95% CL	68% CL	95% CL	value	p-value
c_{HG}	[−0.004, 0.004]	[−0.007, 0.008]	[−0.005, 0.003]	[−0.008, 0.007]	−0.001	0.79
c_{uH}	[−8, 20]	[−14, 26]	[−12, 6]	[−18, 30]	−6, 18	0.50
c_{HW}	[−1.6, 0.9]	[−2.9, 1.6]	[−1.5, 1.3]	[−3.4, 2.1]	0.5	0.66
c_{HB}	[−0.43, 0.38]	[−0.62, 0.60]	[−0.42, 0.37]	[−0.62, 0.59]	−0.03	0.98
c_{HWB}	[−0.75, 0.63]	[−1.09, 0.99]	[−0.71, 0.63]	[−1.06, 0.99]	0.1	0.93
$c_{H\tilde{G}}$	[−0.022, 0.022]	[−0.031, 0.031]	[−0.019, 0.019]	[−0.029, 0.029]	0.000	1.00
$c_{\tilde{u}H}$	[−26, 26]	[−40, 40]	[−37, 37]	[−50, 50]	±21	0.48
$c_{H\widetilde{W}}$	[−1.3, 1.3]	[−2.1, 2.1]	[−1.5, 1.5]	[−2.4, 2.4]	±0.6	0.84
$c_{H\tilde{B}}$	[−0.39, 0.39]	[−0.57, 0.57]	[−0.37, 0.37]	[−0.56, 0.56]	0.00	1.00
$c_{H\widetilde{W}B}$	[−0.71, 0.71]	[−1.05, 1.05]	[−0.69, 0.69]	[−1.03, 1.03]	0.0	1.00

- The constraints are placed on possible CP-even and CP-odd BSM interactions.
- As a result, the data are found to be consistent with the SM hypothesis.

HIGG-2018-28

Combined CMS EFT measurements

- Combined measurements of the production and decay rates of the Higgs boson and its couplings to vector bosons and fermions, and interpretations in the EFT framework were performed.
- The acceptance is assumed to be the same as that predicted in the SM.
- The signal strength values are parameterized in terms of EFT.

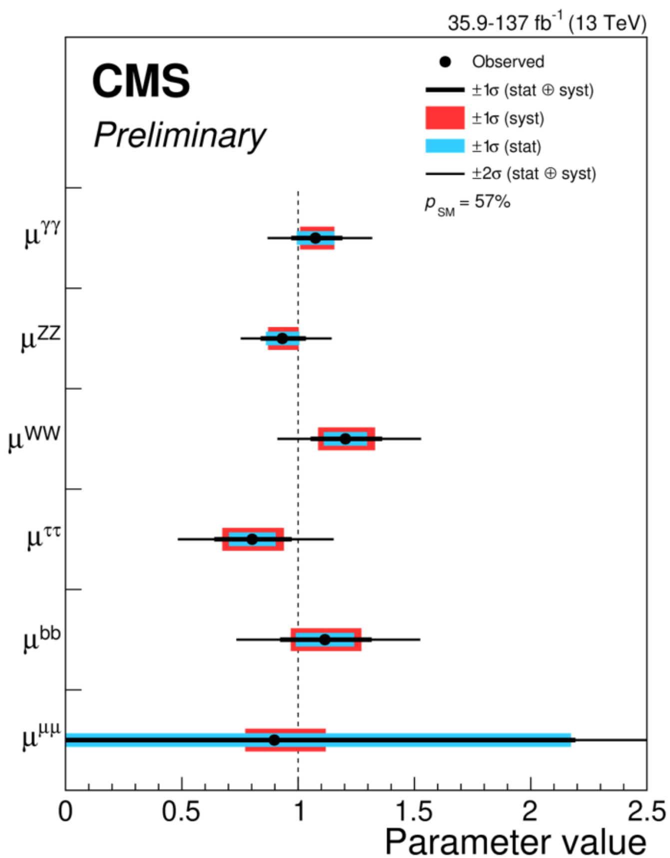

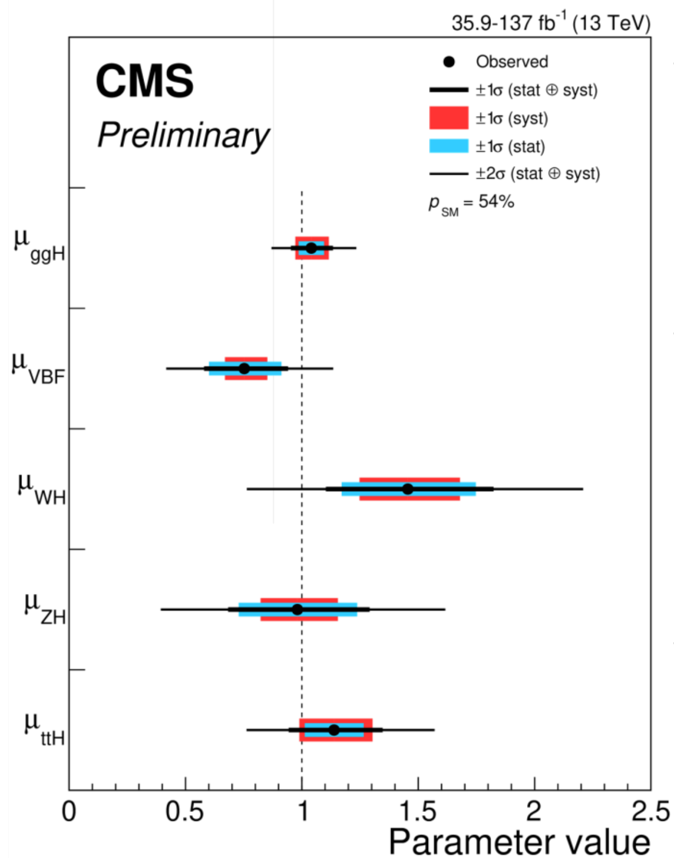

- The STXS interpretation was done within the Higgs Effective Lagrangian (HEL) model.
- The HEL Lagrangian adds 39 flavor independent dimension-6 operators:

$$\mathcal{L}_{\rm HEL} = \mathcal{L}_{\rm SM} + \sum_j \mathcal{O}_j f_j / \Lambda^2$$

- New physics $\sim f_j/\Lambda^2$.

HIG-19-005

Combined CMS EFT measurements

- Cor … gs to vec…
- The … ion was … Higgs … (HEL)
- The … adds … endent … rs: … $_j f_j/\Lambda^2$ …

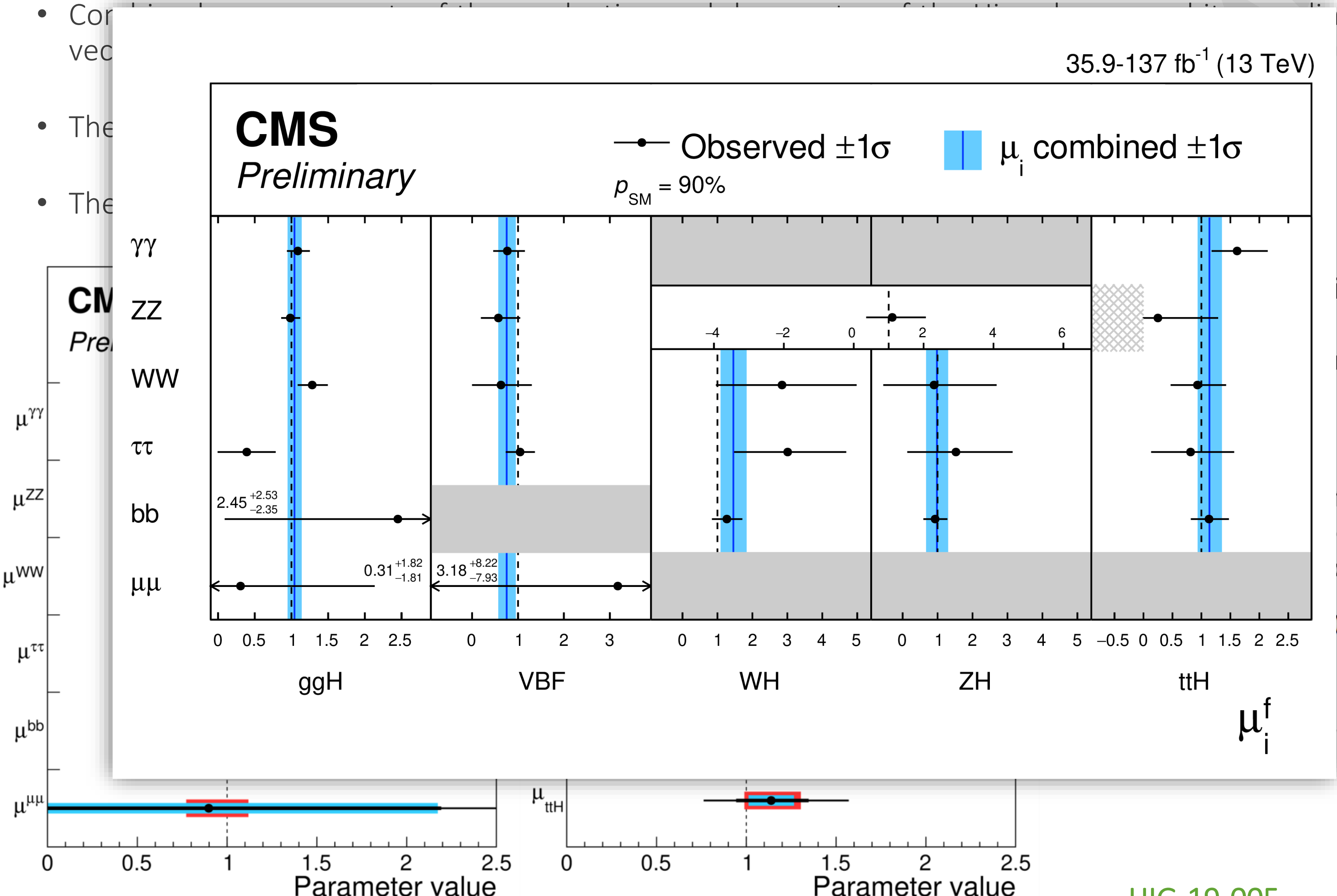

HIG-19-005

Combined CMS EFT measurements

- Signal strength measurements were interpreted in terms of HEL EFT framework.
- Only leading CP-even terms were considered, which are not tightly constrained by other data.
- CP-odd parameters are neglected – not present at the leading order in $1/\Lambda^2$. The CP-even quadratic terms are also assumed to be small.

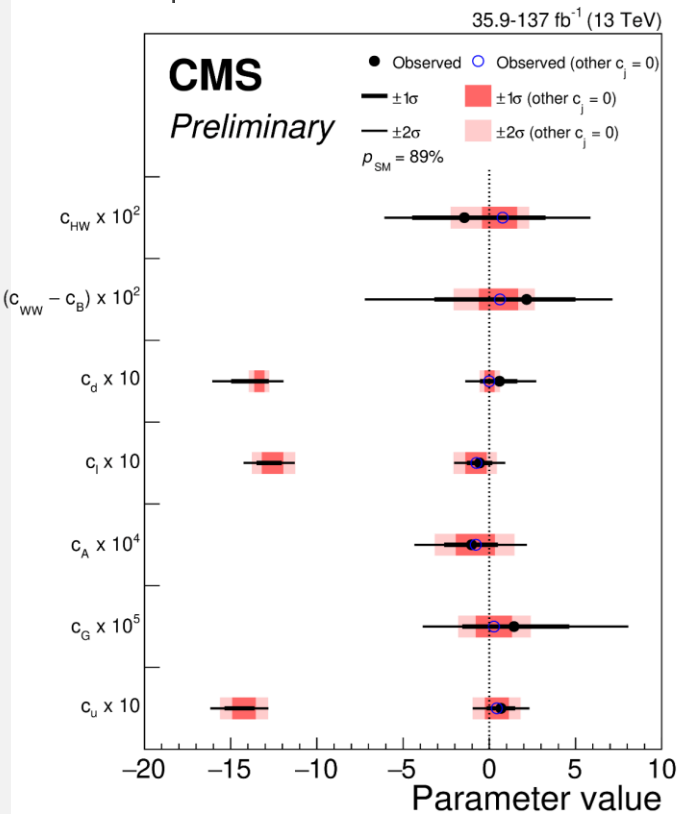

HEL Parameters	Definition	Others profiled	Fix others to SM
$c_A \times 10^4$	$c_A = \frac{m_W^2}{g'^2}\frac{f_A}{\Lambda^2}$	$-1.03^{+1.53}_{-1.59}$ $\left(^{+1.59}_{-1.56}\right)$	$-0.78^{+1.11}_{-1.16}$ $\left(^{+1.10}_{-1.11}\right)$
$c_G \times 10^5$	$c_G = \frac{m_W^2}{g_s^2}\frac{f_G}{\Lambda^2}$	$1.43^{+3.20}_{-3.00}$ $\left(^{+3.13}_{-2.74}\right)$	$0.27^{+1.05}_{-1.05}$ $\left(^{+1.03}_{-1.01}\right)$
$c_u \times 10$	$c_u = -v^2\frac{f_u}{\Lambda^2}$	$0.68^{+0.82}_{-0.83}$ $\left(^{+0.83}_{-0.79}\right)$	$0.43^{+0.69}_{-0.69}$ $\left(^{+0.68}_{-0.67}\right)$
$c_d \times 10$	$c_d = -v^2\frac{f_d}{\Lambda^2}$	$0.59^{+1.03}_{-1.13}$ $\left(^{+1.08}_{-1.05}\right)$	$-0.01^{+0.31}_{-0.28}$ $\left(^{+0.30}_{-0.28}\right)$
$c_\ell \times 10$	$c_\ell = -v^2\frac{f_\ell}{\Lambda^2}$	$-0.57^{+0.74}_{-0.73}$ $\left(^{+0.72}_{-0.77}\right)$	$-0.75^{+0.60}_{-0.64}$ $\left(^{+0.58}_{-0.60}\right)$
$c_{HW} \times 10^2$	$c_{HW} = \frac{m_W^2}{2g}\frac{f_{HW}}{\Lambda^2}$	$-1.45^{+4.72}_{-3.03}$ $\left(^{+3.93}_{-3.27}\right)$	$0.77^{+0.84}_{-1.20}$ $\left(^{+1.04}_{-1.38}\right)$
$(c_{WW} - c_B) \times 10^2$	$c_{WW} = \frac{m_W^2}{g}\frac{f_{WW}}{\Lambda^2}, c_B = \frac{2m_W^2}{g'}\frac{f_B}{\Lambda^2}$	$2.16^{+2.84}_{-5.35}$ $\left(^{+3.46}_{-5.00}\right)$	$0.62^{+1.06}_{-1.22}$ $\left(^{+1.09}_{-1.23}\right)$

- All results are found to be compatible with the standard model expectation within the current uncertainties.

HIG-19-005

EFT measurements in the $\gamma\gamma$ channel (ATLAS)

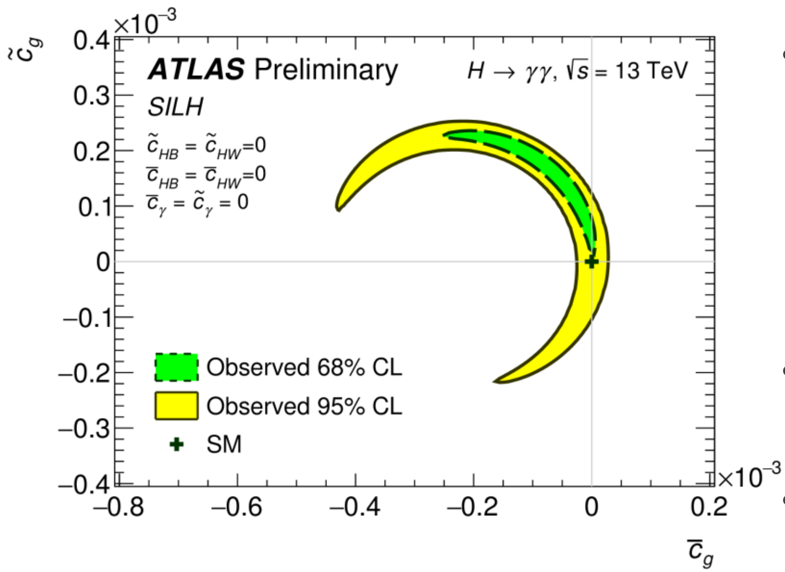

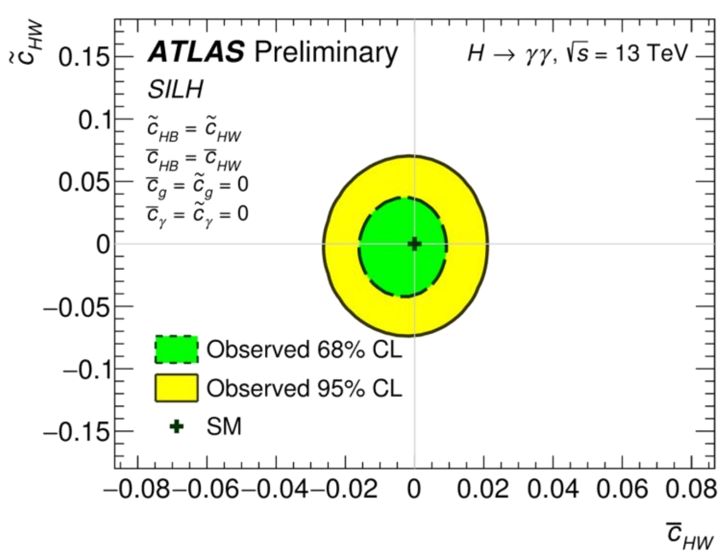

- Measurements of the fiducial integrated and differential cross sections for the $\gamma\gamma$ mode.

Objects	Fiducial definition
Photons	$\lvert\eta\rvert < 2.37$ (excluding $1.37 < \lvert\eta\rvert < 1.52$), $\sum p_T^i / p_T^\gamma < 0.05$
Jets	anti-k_t, $R = 0.4$, $p_T > 30$ GeV, $\lvert y\rvert < 4.4$
Diphoton	$N_\gamma \geq 2$, $105\, GeV < m_{\gamma\gamma} < 160\, GeV$, $p_T^{\gamma_1}/m_{\gamma\gamma} > 0.35$, $p_T^{\gamma_2}/m_{\gamma\gamma} > 0.25$

- EFT interpretation of differential cross sections with CP-even and CP-odd interactions.

- Effective Lagrangian - SILH formulation:

$$\mathcal{L}_{\text{eff}}^{\text{SILH}} \supset \quad \bar{c}_g O_g + \bar{c}_\gamma O_\gamma + \bar{c}_{HW} O_{HW} + \bar{c}_{HB} O_{HB} + \tilde{c}_g \widetilde{O}_g + \tilde{c}_\gamma \widetilde{O}_\gamma + \tilde{c}_{HW} \widetilde{O}_{HW} + \tilde{c}_{HB} \widetilde{O}_{HB}$$

- Effective Lagrangian - SMEFT formulation:

$$\mathcal{L}_{\text{eff}}^{\text{SMEFT}} \supset \quad \overline{C}_{HG} O'_g + \overline{C}_{HW} O'_{HW} + \overline{C}_{HB} O'_{HB} + \overline{C}_{HWB} O'_{HWB} + \widetilde{C}_{HG} \widetilde{O}'_g + \widetilde{C}_{HW} \widetilde{O}'_{HW} + \widetilde{C}_{HB} \widetilde{O}'_{HB} + \widetilde{C}_{HWB} \widetilde{O}'_{HWB}$$

  - CP-conserving: $\bar{C}_{HG}$, $\bar{C}_{HW}$, $\bar{C}_{HB}$ and $\bar{C}_{HWB}$.
  - CP-violating: $\tilde{C}_{HG}$, $\tilde{C}_{HW}$, $\tilde{C}_{HB}$ and $\tilde{C}_{HWB}$.

ATLAS-CONF-2019-029

EFT measurements in the $\gamma\gamma$ channel (ATLAS)

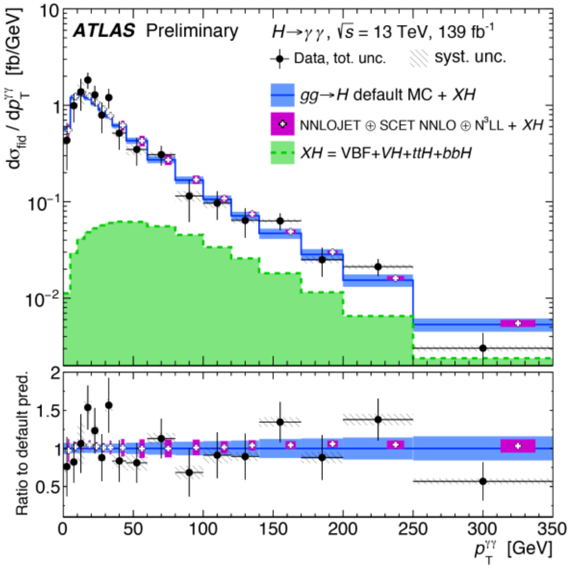

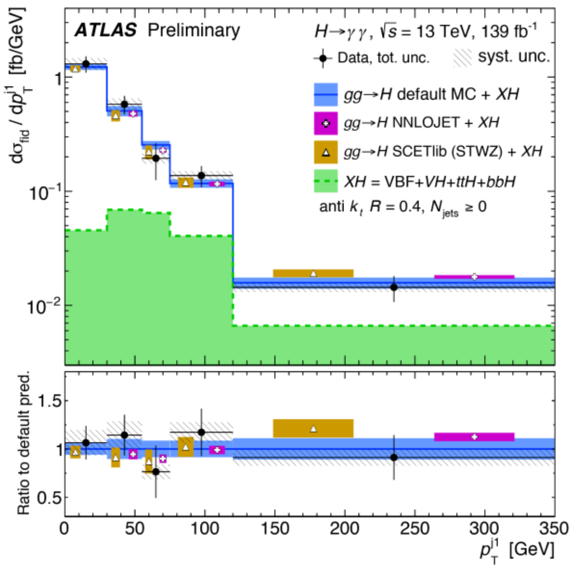

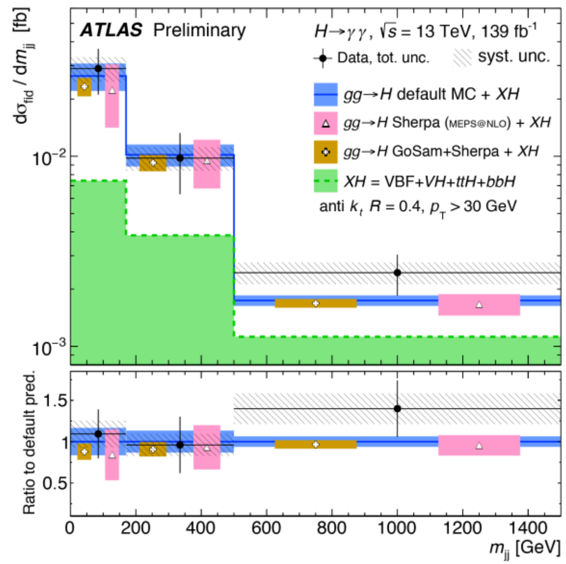

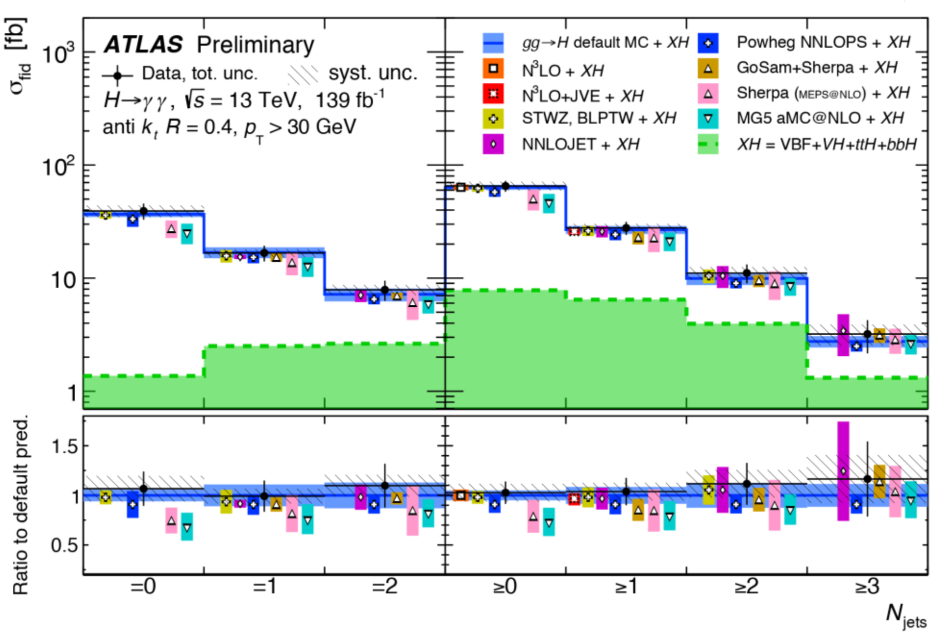

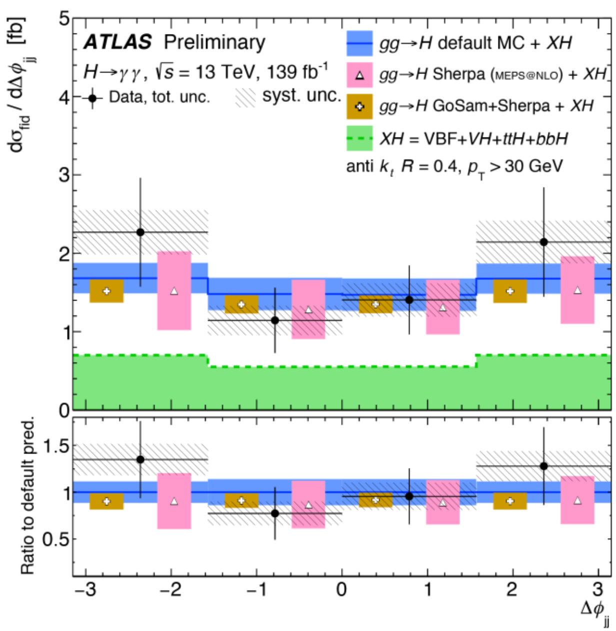

EFT measurements in the $\gamma\gamma$ channel (ATLAS)

- Limits on Wilson coefficients are set with the differential cross sections:

$$\mathcal{L} = \frac{1}{\sqrt{(2\pi)^k\,|C|}} \exp\left(-\frac{1}{2}\left(\vec{\sigma}_{\text{data}} - \vec{\sigma}_{\text{pred}}\right)^T C^{-1} \left(\vec{\sigma}_{\text{data}} - \vec{\sigma}_{\text{pred}}\right)\right)$$

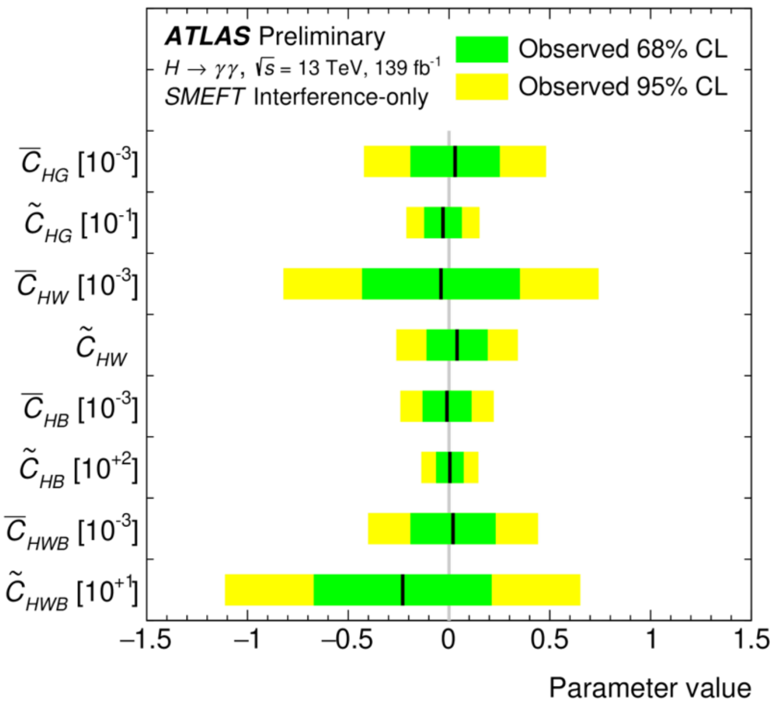

- Fitting one Wilson coefficient at a time.
- Five analyzed observables: $p_T^{\gamma\gamma}$, p_T^{j1}, N_{jets}, m_{jj} and $\Delta\varphi_{jj}$.
- Results have improved by a factor of two in comparison to the previous measurement.

SILH basis:

Coefficient	Observed 95% CL limit	Expected 95% CL limit
$\bar{c}_g$	$[-0.26, 0.26] \times 10^{-4}$	$[-0.25, 0.25] \cup [-4.7, -4.3] \times 10^{-4}$
$\tilde{c}_g$	$[-1.3, 1.1] \times 10^{-4}$	$[-1.1, 1.1] \times 10^{-4}$
$\bar{c}_{HW}$	$[-2.5, 2.2] \times 10^{-2}$	$[-3.0, 3.0] \times 10^{-2}$
$\tilde{c}_{HW}$	$[-6.5, 6.3] \times 10^{-2}$	$[-7.0, 7.0] \times 10^{-2}$
$\bar{c}_\gamma$	$[-1.1, 1.1] \times 10^{-4}$	$[-1.0, 1.2] \times 10^{-4}$
$\tilde{c}_\gamma$	$[-2.8, 4.3] \times 10^{-4}$	$[-2.9, 3.8] \times 10^{-4}$

SMEFT basis:

Coefficient	95% CL, interference-only terms	95% CL, interference and quadratic terms
$\overline{C}_{HG}$	$[-4.2, 4.8] \times 10^{-4}$	$[-6.1, 4.7] \times 10^{-4}$
$\widetilde{C}_{HG}$	$[-2.1, 1.6] \times 10^{-2}$	$[-1.5, 1.4] \times 10^{-3}$
$\overline{C}_{HW}$	$[-8, 2, 7.4] \times 10^{-4}$	$[-8.3, 8.3] \times 10^{-4}$
$\widetilde{C}_{HW}$	$[-0.26, 0.33]$	$[-3.7, 3.7] \times 10^{-3}$
$\overline{C}_{HB}$	$[-2.4, 2.3] \times 10^{-4}$	$[-2.4, 2.4] \times 10^{-4}$
$\widetilde{C}_{HB}$	$[-13.0, 14.0]$	$[-1.2, 1.1] \times 10^{-3}$
$\overline{C}_{HWB}$	$[-4.0, 4.4] \times 10^{-4}$	$[-4.2, 4.2] \times 10^{-4}$
$\widetilde{C}_{HWB}$	$[-11.1, 6.5]$	$[-2.0, 2.0] \times 10^{-3}$

- The measurements and are found to be in good agreement with the Standard Model predictions.

ATLAS-CONF-2019-029

EFT measurements in the $\tau\tau$ and $4l$ channels (CMS)

- A study of anomalous HVV interactions was performed.
- Production: ggF and VBF.
- Decay: $\tau\tau$.
- Combination with $H \rightarrow 4l$ analysis.
- Anomalous interactions are parametrized by a scattering amplitude:

$$A(\mathrm{HVV}) \sim \left[a_1^{\mathrm{VV}} + \frac{\kappa_1^{\mathrm{VV}} q_1^2 + \kappa_2^{\mathrm{VV}} q_2^2}{\left(\Lambda_1^{\mathrm{VV}}\right)^2} \right] m_{\mathrm{V}1}^2 \epsilon_{\mathrm{V}1}^* \epsilon_{\mathrm{V}2}^* + a_2^{\mathrm{VV}} f_{\mu\nu}^{*(1)} f^{*(2)\mu\nu} + a_3^{\mathrm{VV}} f_{\mu\nu}^{*(1)} \tilde{f}^{*(2)\mu\nu}$$

- The results are consistent with the standard model expectations.

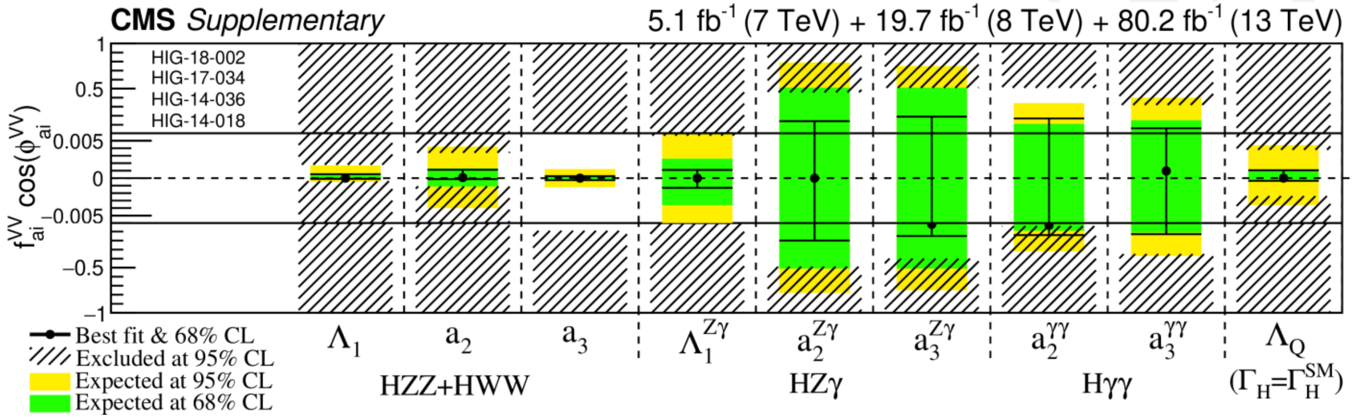

Parameter	Observed / (10^{-3})		Expected / (10^{-3})	
	68% CL	95% CL	68% CL	95% CL
$f_{a3}\cos(\phi_{a3})$	0.00 ± 0.27	$[-92, 14]$	0.00 ± 0.23	$[-1.2, 1.2]$
$f_{a2}\cos(\phi_{a2})$	$0.08^{+1.04}_{-0.21}$	$[-1.1, 3.4]$	$0.0^{+1.3}_{-1.1}$	$[-4.0, 4.2]$
$f_{\Lambda1}\cos(\phi_{\Lambda1})$	$0.00^{+0.53}_{-0.09}$	$[-0.4, 1.8]$	$0.00^{+0.48}_{-0.12}$	$[-0.5, 1.7]$
$f_{\Lambda1}^{Z\gamma}\cos(\phi_{\Lambda1}^{Z\gamma})$	$0.0^{+1.1}_{-1.3}$	$[-6.5, 5.7]$	$0.0^{+2.6}_{-3.6}$	$[-11, 8.0]$

Parameter	Observed	Expected
a_3/a_1	$[-0.81, 0.31]$	$[-0.090, 0.090]$
a_2/a_1	$[-0.055, 0.097]$	$[-0.11, 0.11]$
$(\Lambda_1\sqrt{\lvert a_1\rvert})\cos(\phi_{\Lambda1})$ (GeV)	$[-\infty, -650] \cup [440, \infty]$	$[-\infty, -610] \cup [450, \infty]$
$(\Lambda_1^{Z\gamma}\sqrt{\lvert a_1\rvert})\cos(\phi_{\Lambda1}^{Z\gamma})$ (GeV)	$[-\infty, -400] \cup [420, \infty]$	$[-\infty, -360] \cup [390, \infty]$

HIG-17-034

Conclusion

- There are 8 years passed since the Higgs boson discovery, but many questions are still requiring answers.
- The Effective Field Theory approach allows to test various BSM hypotheses in different production and decay channels of the Higgs boson.
- Series of STXS and EFT ATLAS and CMS analyses were performed in order to find possible traces of BSM physics.
- <u>As for now, no significant deviations from the Standard Model were observed.</u>
- New, more strict limits were placed on the EFT parameters.


Thank You

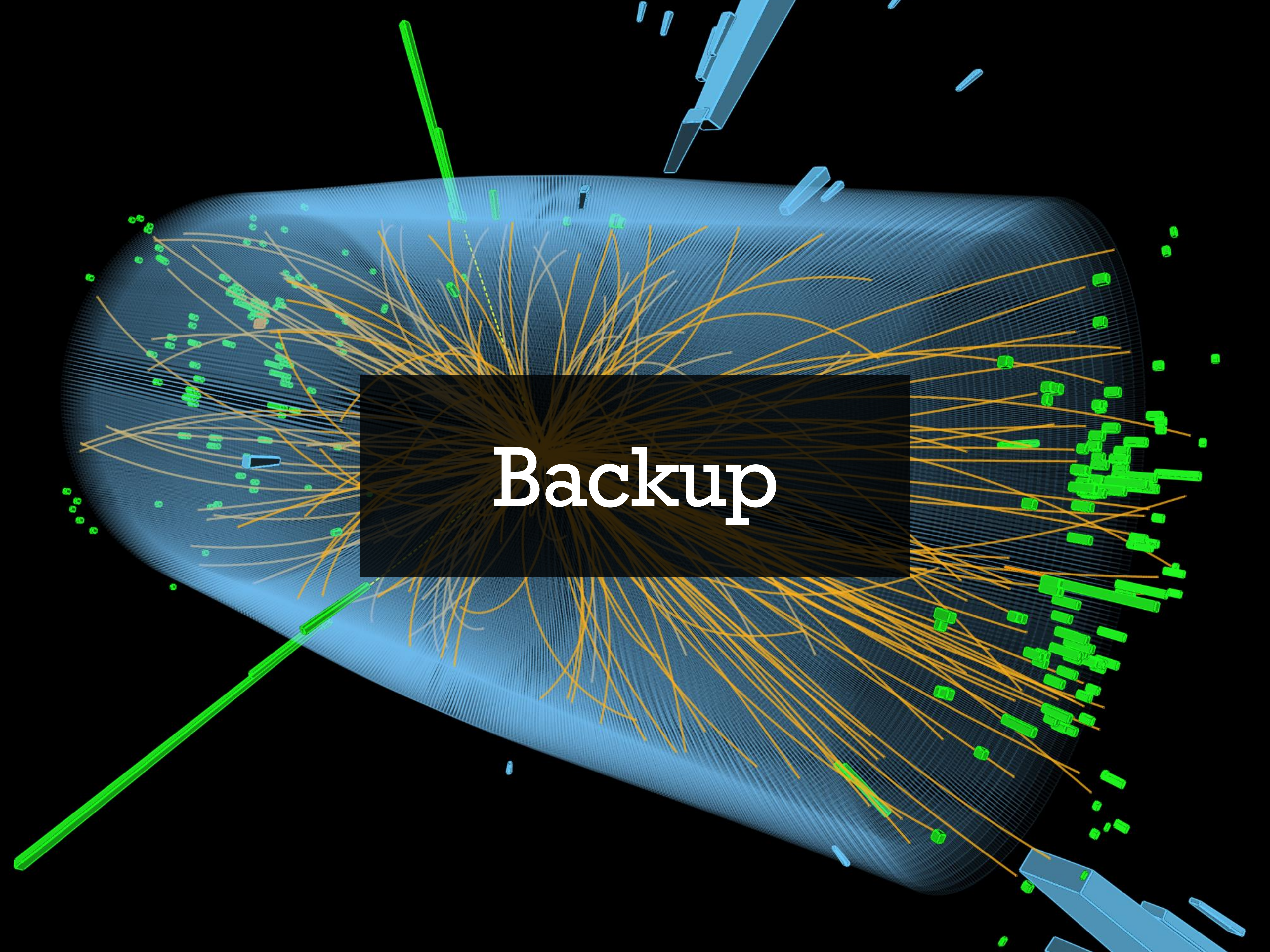

Backup

SILH basis and Higgs Effective Lagrangian (HEL)

- CP-conserving operators (SILH basis - the main part of HEL):

$$\begin{aligned}
\mathcal{L}_{\text{SILH}} = &\frac{\bar{c}_H}{2v^2}\partial^\mu\left[\Phi^\dagger\Phi\right]\partial_\mu\left[\Phi^\dagger\Phi\right] + \frac{\bar{c}_T}{2v^2}\left[\Phi^\dagger \overleftrightarrow{D}^\mu \Phi\right]\left[\Phi^\dagger \overleftrightarrow{D}_\mu \Phi\right] - \frac{\bar{c}_6\lambda}{v^2}\left[\Phi^\dagger\Phi\right]^3 \\
&- \left[\frac{\bar{c}_u}{v^2} y_u \Phi^\dagger\Phi\ \Phi^\dagger\cdot\bar{Q}_L u_R + \frac{\bar{c}_d}{v^2} y_d \Phi^\dagger\Phi\ \Phi\bar{Q}_L d_R + \frac{\bar{c}_l}{v^2} y_\ell\ \Phi^\dagger\Phi\ \Phi\bar{L}_L e_R + \text{h.c.}\right] \\
&+ \frac{ig\ \bar{c}_W}{m_W^2}\left[\Phi^\dagger T_{2k} \overleftrightarrow{D}^\mu \Phi\right] D^\nu W^k_{\mu\nu} + \frac{ig'\ \bar{c}_B}{2m_W^2}\left[\Phi^\dagger \overleftrightarrow{D}^\mu \Phi\right]\partial^\nu B_{\mu\nu} \\
&+ \frac{2ig\ \bar{c}_{HW}}{m_W^2}\left[D^\mu\Phi^\dagger T_{2k} D^\nu\Phi\right] W^k_{\mu\nu} + \frac{ig'\ \bar{c}_{HB}}{m_W^2}\left[D^\mu\Phi^\dagger D^\nu\Phi\right] B_{\mu\nu} \\
&+ \frac{g'^2\ \bar{c}_\gamma}{m_W^2}\Phi^\dagger\Phi B_{\mu\nu}B^{\mu\nu} + \frac{g_s^2\ \bar{c}_g}{m_W^2}\Phi^\dagger\Phi G^a_{\mu\nu}G_a^{\mu\nu}\ ,
\end{aligned}$$

- CP-violating operators (additional part of HEL):

$$\begin{aligned}
\mathcal{L}_{CP} = &\frac{ig\ \tilde{c}_{HW}}{m_W^2} D^\mu\Phi^\dagger T_{2k} D^\nu\Phi \widetilde{W}^k_{\mu\nu} + \frac{ig'\ \tilde{c}_{HB}}{m_W^2} D^\mu\Phi^\dagger D^\nu\Phi \widetilde{B}_{\mu\nu} + \frac{g'^2\ \tilde{c}_\gamma}{m_W^2}\Phi^\dagger\Phi B_{\mu\nu}\widetilde{B}^{\mu\nu} \\
&+ \frac{g_s^2\ \tilde{c}_g}{m_W^2}\Phi^\dagger\Phi G^a_{\mu\nu}\widetilde{G}_a^{\mu\nu} + \frac{g^3\ \tilde{c}_{3W}}{m_W^2}\epsilon_{ijk} W^i_{\mu\nu} W^{\nu j}{}_\rho \widetilde{W}^{\rho\mu k} + \frac{g_s^3\ \tilde{c}_{3G}}{m_W^2} f_{abc} G^a_{\mu\nu} G^{\nu b}{}_\rho \widetilde{G}^{\rho\mu c}
\end{aligned}$$

- Higgs Effective Lagrangian:

$$\mathcal{L} = \mathcal{L}_{\text{SM}} + \sum \bar{c}_i \mathcal{O}_i = \mathcal{L}_{\text{SM}} + \mathcal{L}_{\text{SILH}} + \mathcal{L}_{CP} + \mathcal{L}_{F_1} + \mathcal{L}_{F_2} + \mathcal{L}_G$$

STXS measurements in the $4l$ channel (CMS)

- The dominant experimental sources of systematics: lepton identification efficiencies and luminosity measurement.
- The dominant theoretical source of systematics: the category migration for the ggH process.

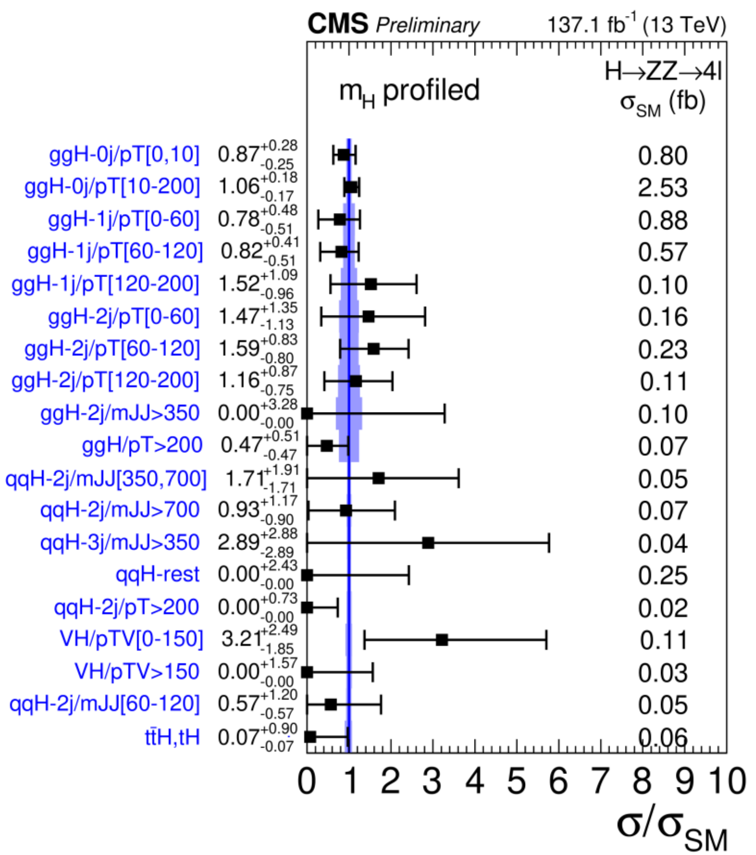

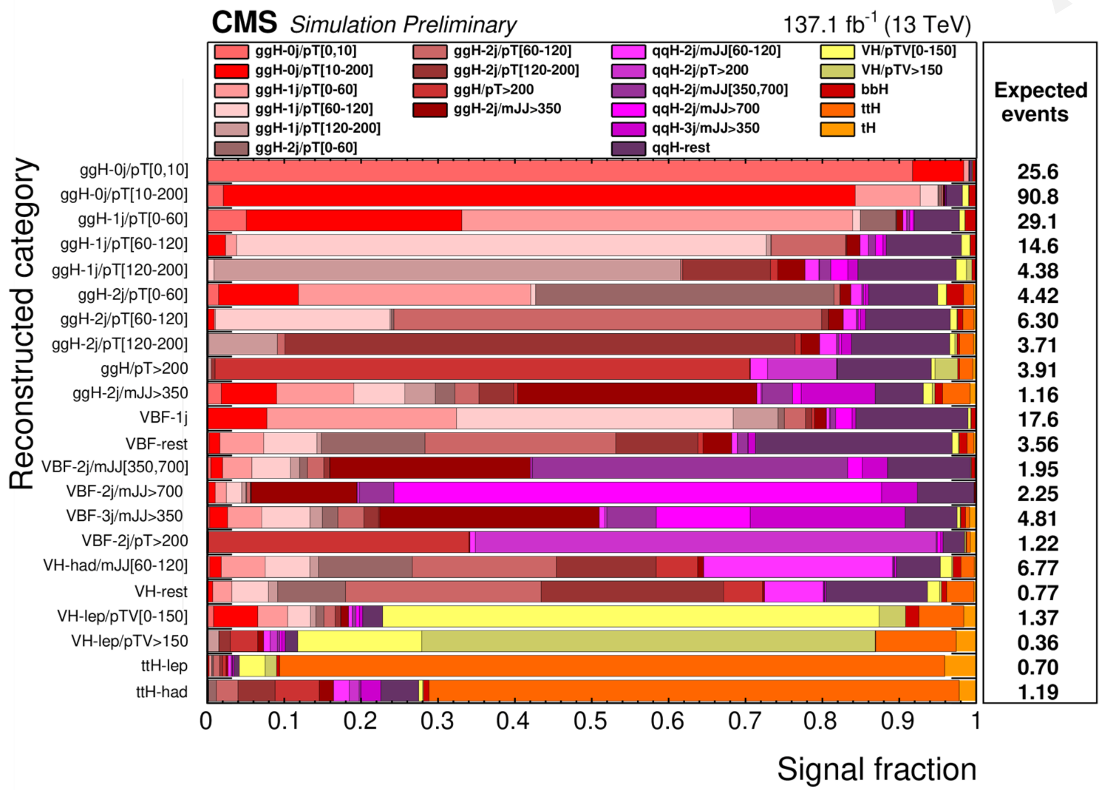

- <u>All results are found to be compatible with the SM predictions, within the measurements precision.</u>

HIG-19-001

STXS measurements in the bb channel (CMS)

- An inclusive search for the SM Higgs boson produced with large p_T and decaying to a bb pair was performed.
- With respect to the previous CMS result, the relative precision of the Higgs boson signal strength measurement improves by approximately a factor of two.
- The measured signal strength is $\mu_H = 3.68 \pm 1.20\ (stat)\ ^{+0.63}_{-0.66}(syst)\ ^{+0.81}_{-0.46}(theo)$.

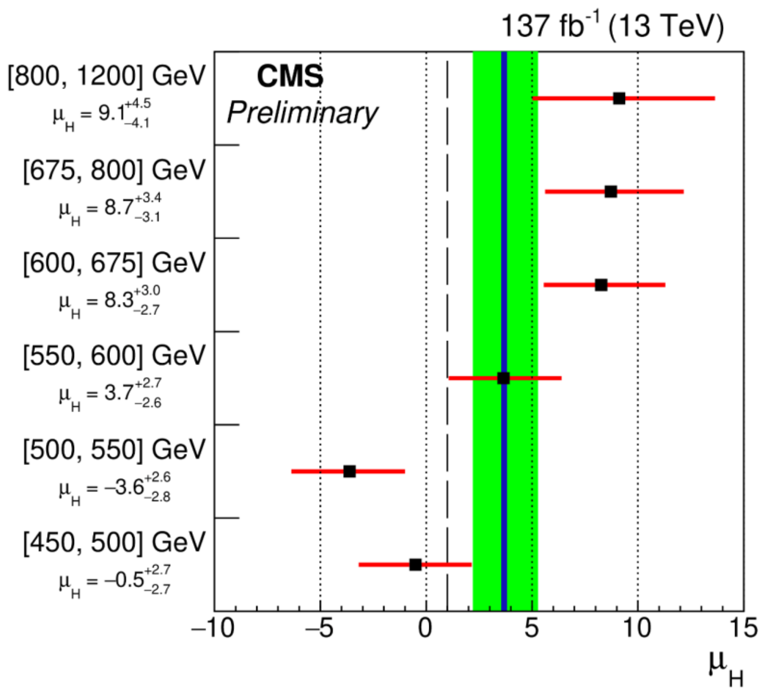

	2016	2017	2018	Combined
Expected signal strength μ_Z	$1.00^{+0.38}_{-0.28}$	$1.00^{+0.42}_{-0.29}$	$1.00^{+0.43}_{-0.29}$	$1.00^{+0.23}_{-0.19}$
Observed signal strength μ_Z	$0.86^{+0.32}_{-0.24}$	$1.11^{+0.48}_{-0.33}$	$0.91^{+0.37}_{-0.26}$	$1.01^{+0.24}_{-0.20}$
HJ-MINLO				
Expected signal strength μ_H	$1.00^{+3.34}_{-3.54}$	$1.00^{+2.46}_{-2.50}$	$1.00^{+2.30}_{-2.37}$	$1.00^{+1.42}_{-1.40}$
Observed signal strength μ_H	$7.92^{+3.42}_{-3.19}$	$4.76^{+2.64}_{-2.47}$	$1.70^{+2.31}_{-2.33}$	$3.68^{+1.58}_{-1.46}$
Expected H significance ($\mu_H = 1$)	0.29σ	0.41σ	0.43σ	0.71σ
Observed H significance	2.42σ	1.90σ	0.73σ	2.54σ
Expected UL signal strength ($\mu_H = 0$)	< 6.84	< 5.02	< 4.67	< 2.90
Observed UL signal strength	< 7.97	< 4.78	< 1.70	< 3.70
Ref. H p_T spectrum				
Expected signal strength μ_H	$1.00^{+1.52}_{-1.50}$	$1.00^{+1.14}_{-1.06}$	$1.00^{+1.12}_{-1.05}$	$1.00^{+0.68}_{-0.58}$
Observed signal strength μ_H	$3.97^{+1.89}_{-1.55}$	$2.18^{+1.37}_{-1.19}$	$1.13^{+1.12}_{-1.06}$	$1.90^{+0.86}_{-0.70}$
Expected H significance ($\mu_H = 1$)	0.68σ	0.94σ	0.95σ	1.73σ
Observed H significance	2.62σ	1.84σ	1.06σ	2.85σ
Expected UL signal strength ($\mu_H = 0$)	< 3.41	< 2.42	< 2.29	< 1.42
Observed UL signal strength	< 4.00	< 2.18	< 1.13	< 1.90

- For a Higgs boson mass of 125 GeV, an excess of events above the expected background is observed with a local significance of 2.54 standard deviations, where the expectation is 0.71.

HIG-19-003

STXS measurements in the bb channel (ATLAS)

- The same measurements were performed with the whole Run II dataset.
- Results of the STXS measurements were already published, but their EFT interpretation is still under the ATLAS collaboration's approval.
- The total uncertainties vary from 30% in the high gauge boson transverse momentum regions to 85% in the low regions.

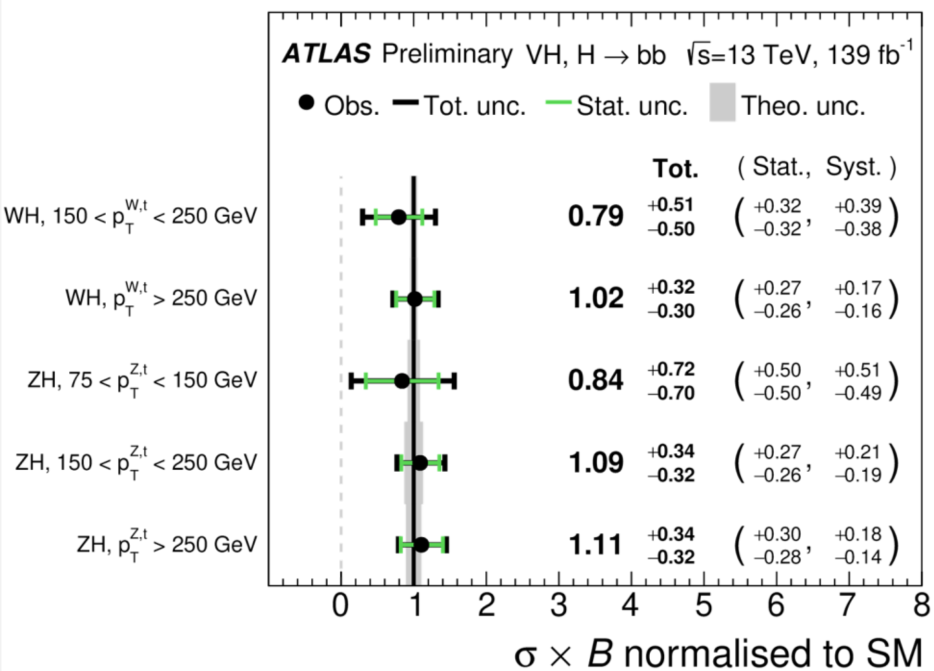

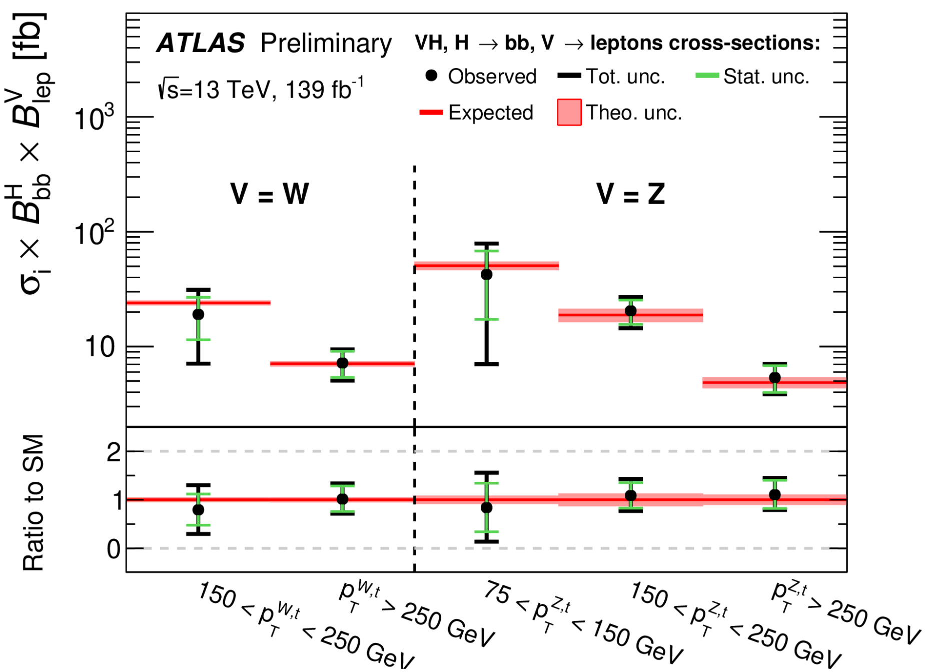

- The cross-section measurements are all consistent with the Standard Model expectations.

ATLAS-CONF-2020-006

STXS measurements in the $4l$ channel (ATLAS)

- Cross-sections times branching ratio are measured for the main Higgs boson production modes in several exclusive phase-space regions with full Run II dataset.
- The dominant Stage 0 experimental systematic uncertainty: lepton efficiency and integrated luminosity measurements. The dominant theoretical uncertainty: parton shower modelling.
- The SM Higgs boson signal is assumed to have a mass $m_H = 125$ GeV .

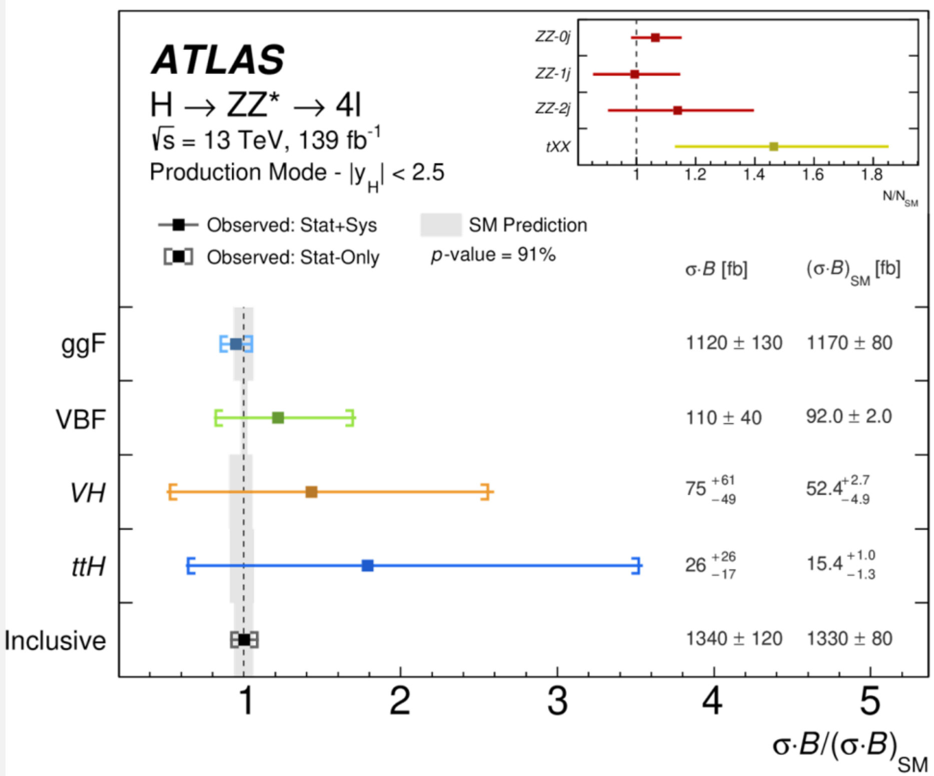

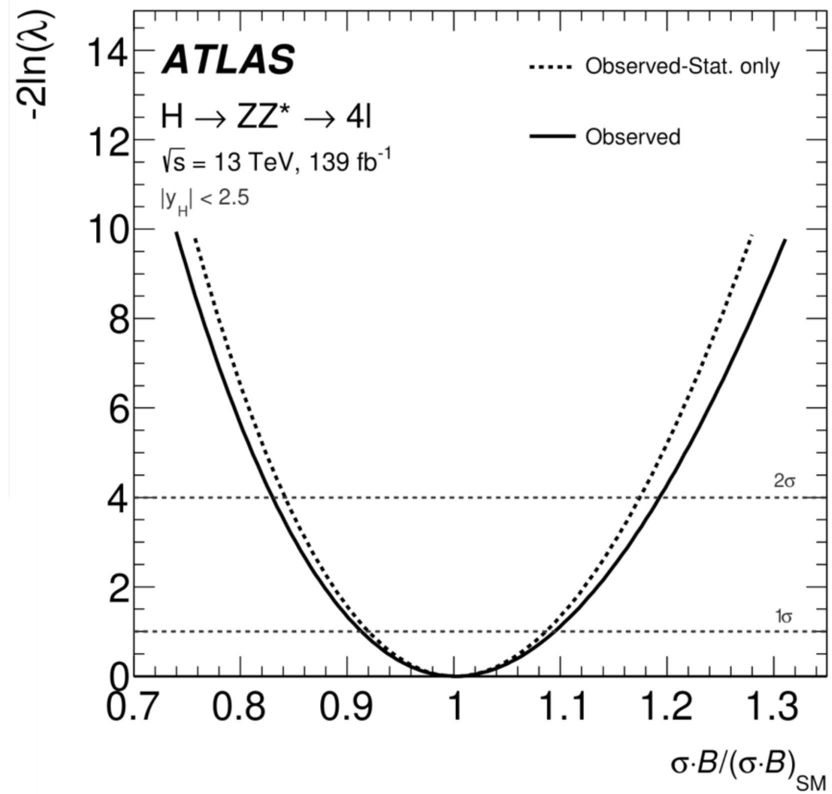

HIGG-2018-28

STXS measurements in the $4l$ channel (ATLAS)

- The dominant Stage 1.1 cross section uncertainties are the jet energy scale and resolution, and parton shower uncertainties.

- By using obtained STXS measurements, exclusion limits are set on the CP-even and CP-odd 'beyond the Standard Model' EFT couplings.

$$\mathcal{B}^{4\ell}(\vec{c}) = \frac{\Gamma^{4\ell}(\vec{c})}{\Gamma^{\text{tot}}(\vec{c})} = \mathcal{B}^{4\ell}_{\text{SM}} \cdot \frac{1 + \sum_i A_i^{4\ell} c_i + \sum_{ij} B_{ij}^{4\ell} c_i c_j}{1 + \sum_f \left(\sum_i A_i^f c_i + \sum_{ij} B_{ij}^f c_i c_j\right)}$$

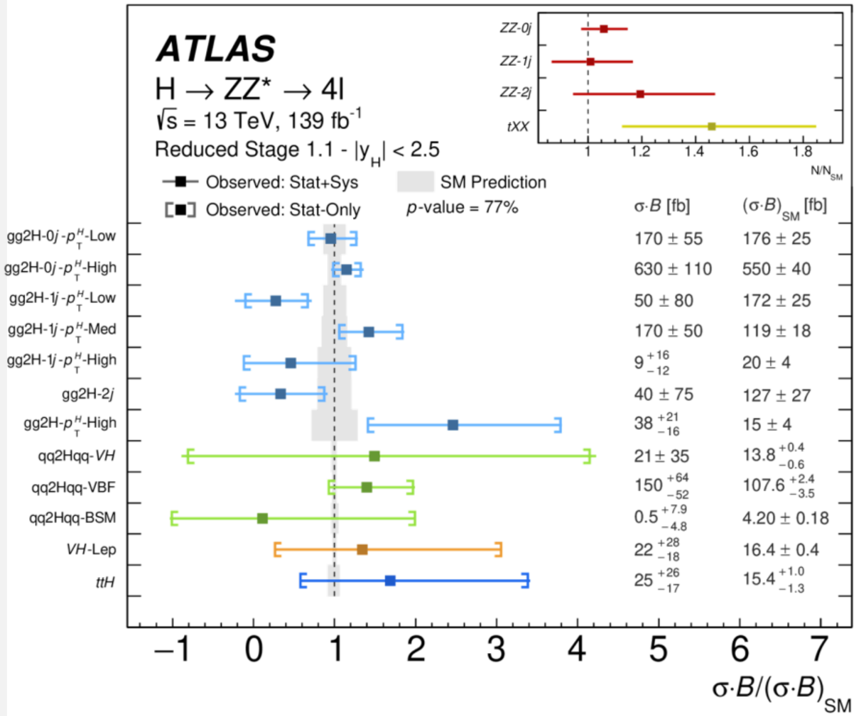

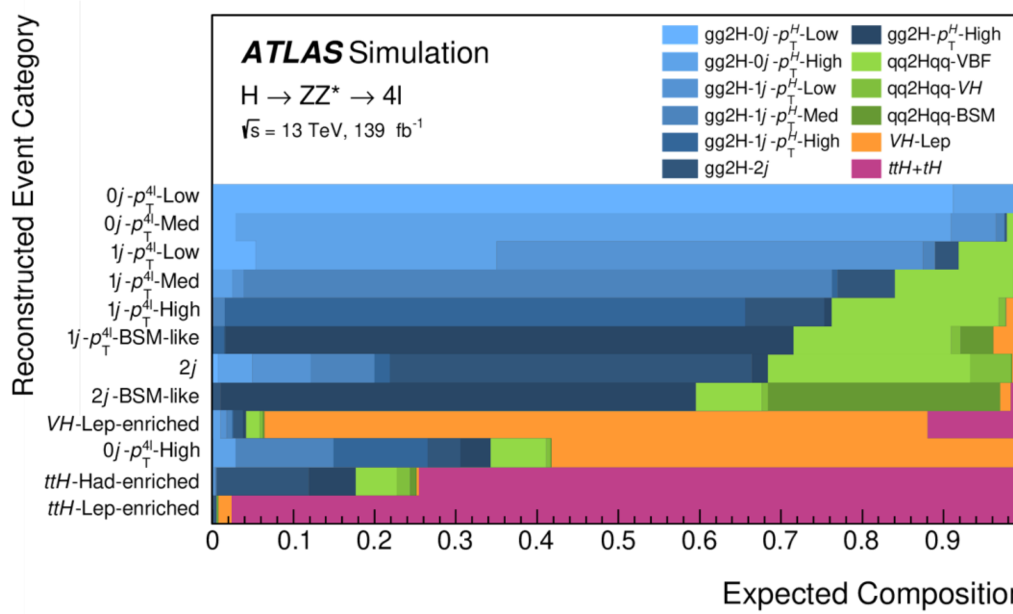

- The measured cross section are in a good agreement with the SM predictions.

HIGG-2018-28

ATLAS $4l$ selection criteria

TRIGGER	
Combination of single-lepton, dilepton and trilepton triggers	
LEPTONS AND JETS	
ELECTRONS	$E_T > 7$ GeV and $\lvert\eta\rvert < 2.47$
MUONS	$p_T > 5$ GeV and $\lvert\eta\rvert < 2.7$, calorimeter-tagged: $p_T > 15$ GeV
JETS	$p_T > 30$ GeV and $\lvert\eta\rvert < 4.5$
QUADRUPLETS	
All combinations of two same-flavour and opposite-charge lepton pairs - Leading lepton pair: lepton pair with invariant mass m_{12} closest to the Z boson mass m_Z - Subleading lepton pair: lepton pair with invariant mass m_{34} second closest to the Z boson mass m_Z Classification according to the decay final state: 4μ, $2e2\mu$, $2\mu 2e$, $4e$	
REQUIREMENTS ON EACH QUADRUPLET	
LEPTON RECONSTRUCTION	- Three highest-p_T leptons must have p_T greater than 20, 15 and 10 GeV - At most one calorimeter-tagged or stand-alone muon
LEPTON PAIRS	- Leading lepton pair: $50 < m_{12} < 106$ GeV - Subleading lepton pair: $m_{\min} < m_{34} < 115$ GeV - Alternative same-flavour opposite-charge lepton pair: $m_{\ell\ell} > 5$ GeV - $\Delta R(\ell, \ell') > 0.10$ for all lepton pairs
LEPTON ISOLATION	- The amount of isolation E_T after summing the track-based and 40% of the calorimeter-based contribution must be smaller than 16% of the lepton p_T
IMPACT PARAMETER SIGNIFICANCE	- Electrons: $\lvert d_0\rvert/\sigma(d_0) < 5$ - Muons: $\lvert d_0\rvert/\sigma(d_0) < 3$
COMMON VERTEX	- χ^2-requirement on the fit of the four lepton tracks to their common vertex
SELECTION OF THE BEST QUADRUPLET	
- Select quadruplet with m_{12} closest to m_Z from one decay final state in decreasing order of priority: 4μ, $2e2\mu$, $2\mu 2e$ and $4e$ - If at least one additional (fifth) lepton with $p_T > 12$ GeV meets the isolation, impact parameter and angular separation criteria, select the quadruplet with the highest matrix-element value	
HIGGS BOSON MASS WINDOW	
- Correction of the four-lepton invariant mass due to the FSR photons in Z boson decays - Four-lepton invariant mass window in the signal region: $115 < m_{4\ell} < 130$ GeV - Four-lepton invariant mass window in the sideband region: $105 < m_{4\ell} < 115$ GeV or $130 < m_{4\ell} < 160$ (350) GeV	

ATLAS $4l$ STXS scheme

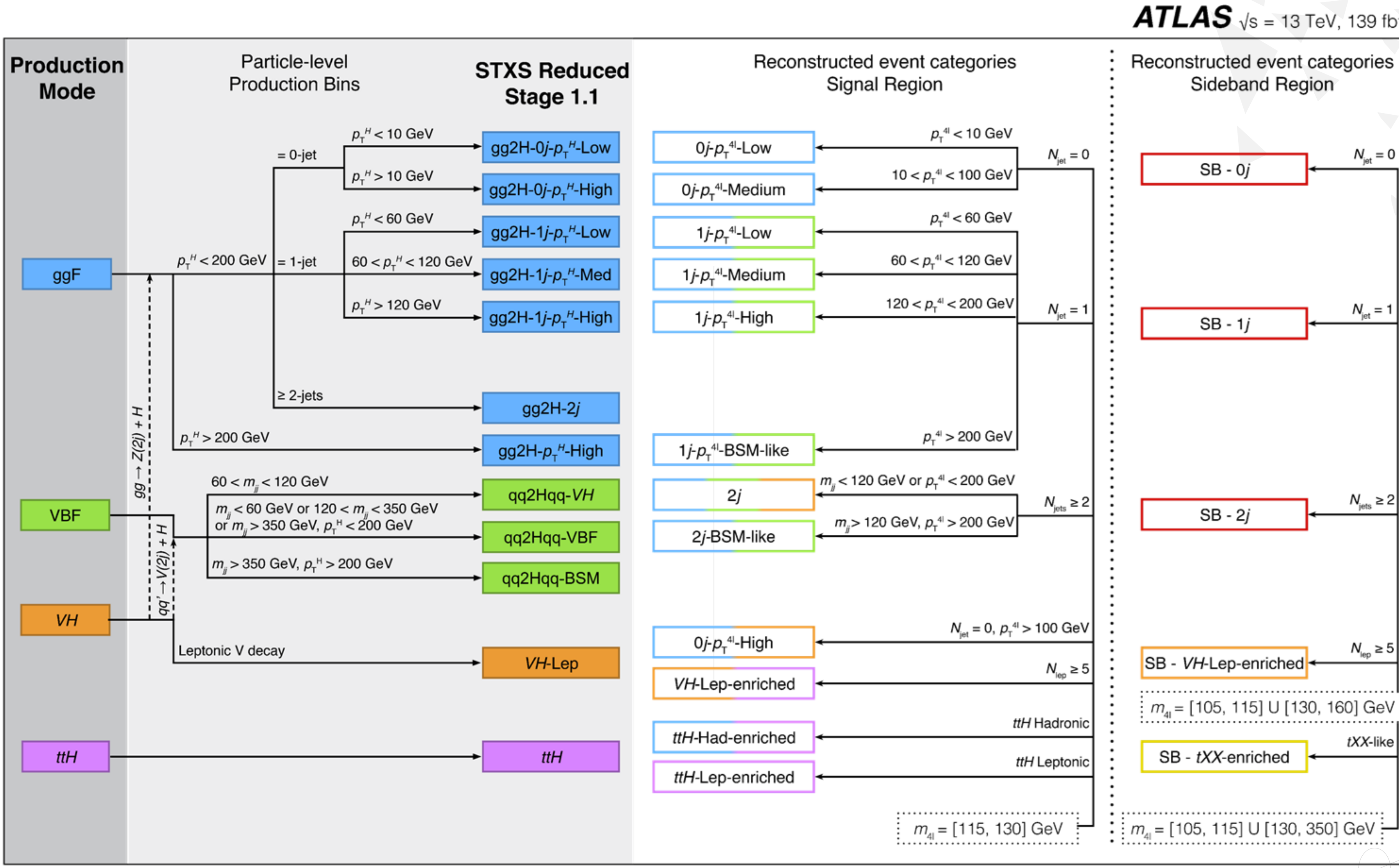

Alternative ATLAS $4l$ STXS scheme

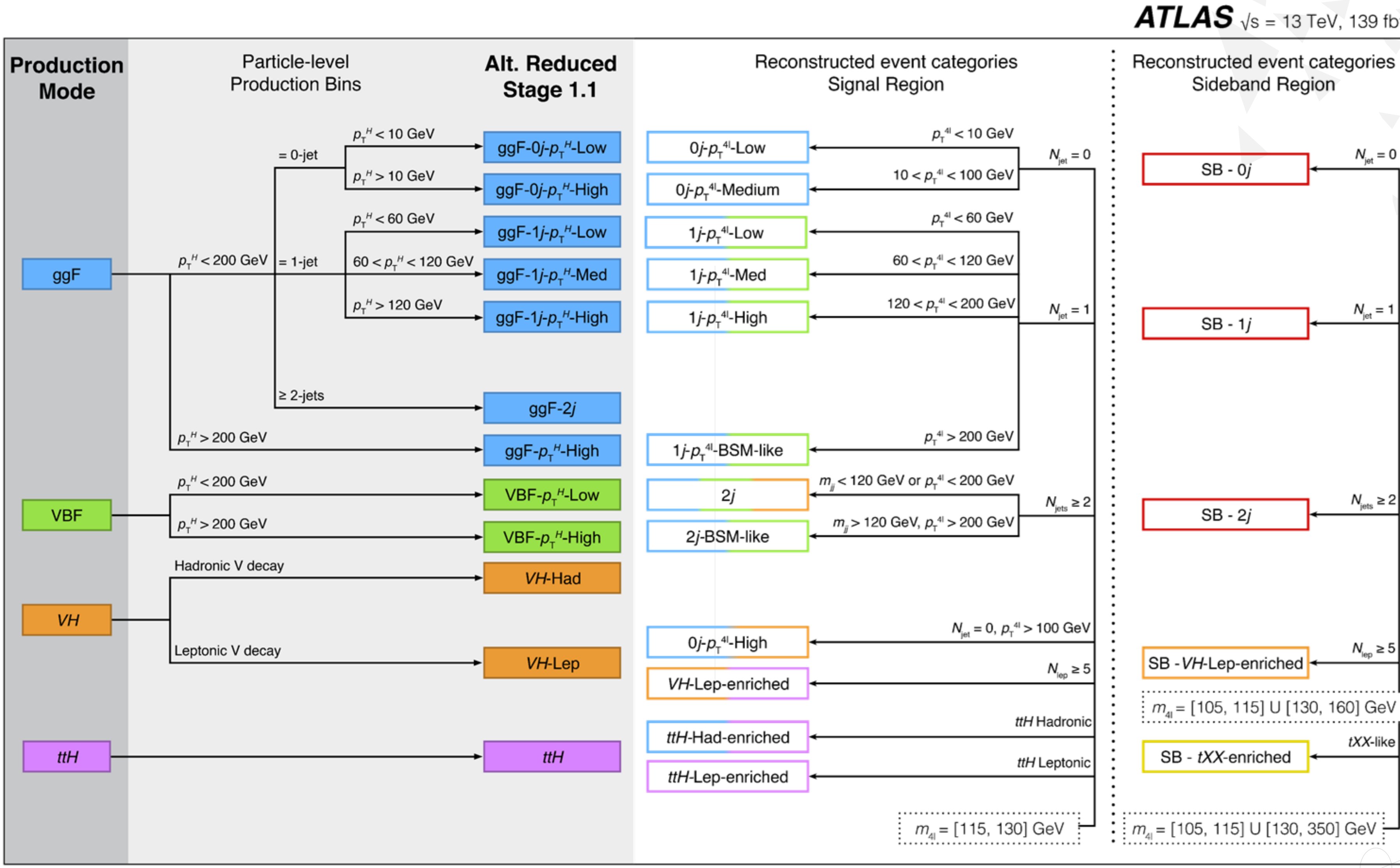

Acceptance in the $4l$ channel (ATLAS)

- The acceptance correction relative to the SM prediction isdescribed by a three-dimensional Lorentzian function with free acceptance parameters $\vec{\alpha}$, $\vec{\beta}$ and $\vec{\delta}$:

$$\frac{A(\vec{c})}{A_{\mathrm{SM}}} = \alpha_0 + (\alpha_1)^2 \cdot \left[\alpha_2 + \sum_i \delta_i \cdot (c_i + \beta_i)^2 + \sum_{\substack{ij \\ i \neq j}} \delta_{(i,j)} \cdot c_i c_j + \delta_{\substack{(i,j,k) \\ i \neq j \neq k}} \cdot c_i c_j c_k \right]^{-1},$$

where indices i, j and k run over (HW, HB, HWB) in case of the acceptance correction for the set of CP-even parameters and over $(H\widetilde{W}, H\tilde{B}, H\widetilde{W}B)$ In case of the CP-odd parameters.

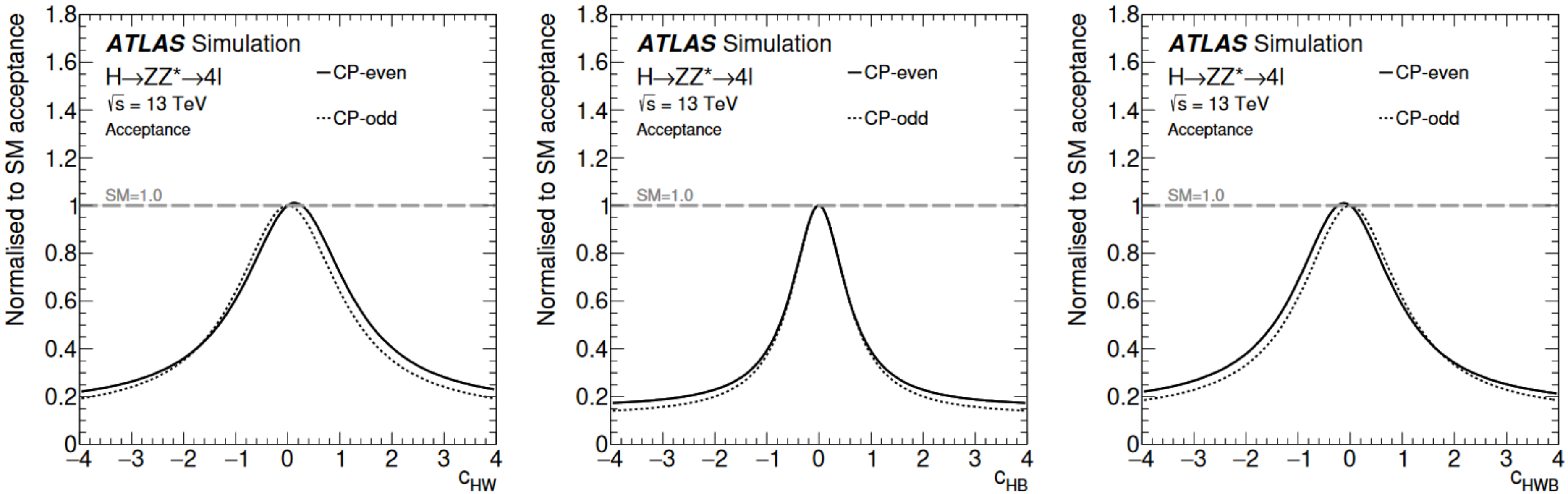

HIGG-2018-28

CMS $4l$ STXS scheme

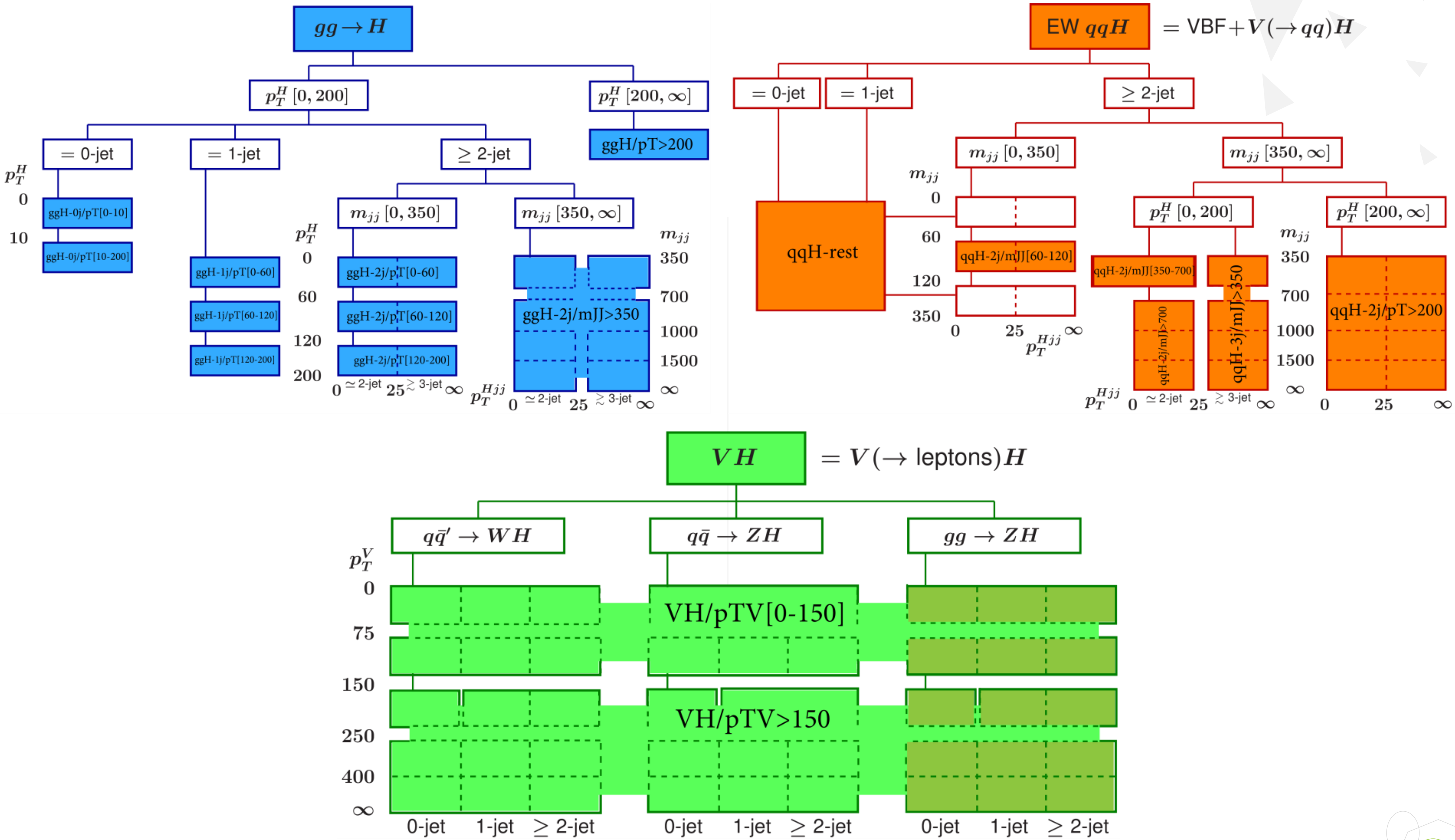

STXS measurements in the $4l$ channel (CMS)

- Properties of the Higgs boson were measured in the $H \to ZZ^* \to 4l$ $(l = e, \mu)$ decay channel.
- The STXS measurements were performed for ggF, VBF, VH and ttH Higgs boson production channels and for different phase space sub-categories.
- The cross section values were obtained assuming the Higgs mass $m_H = 125.1$ GeV (best fit mass value).

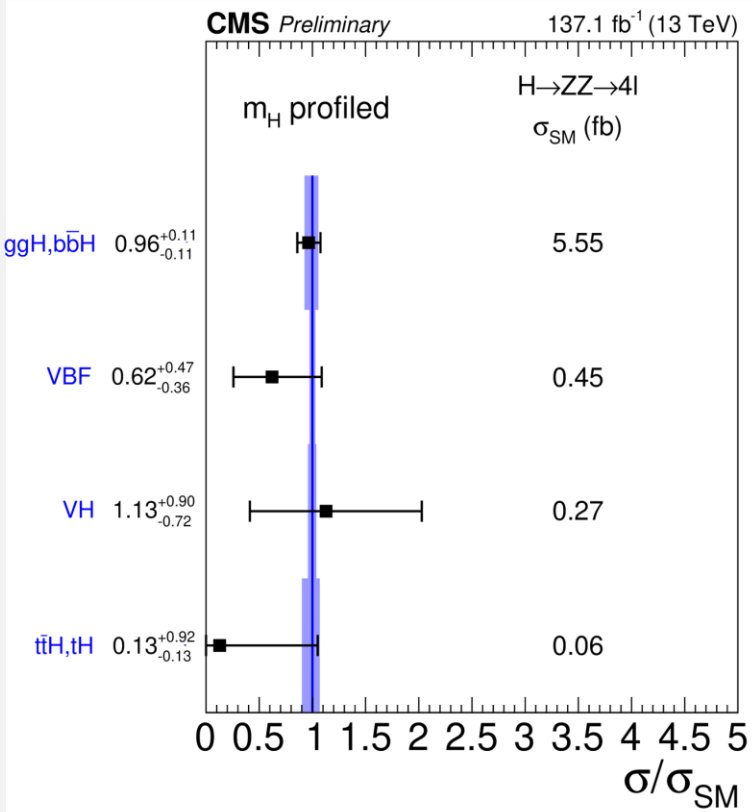

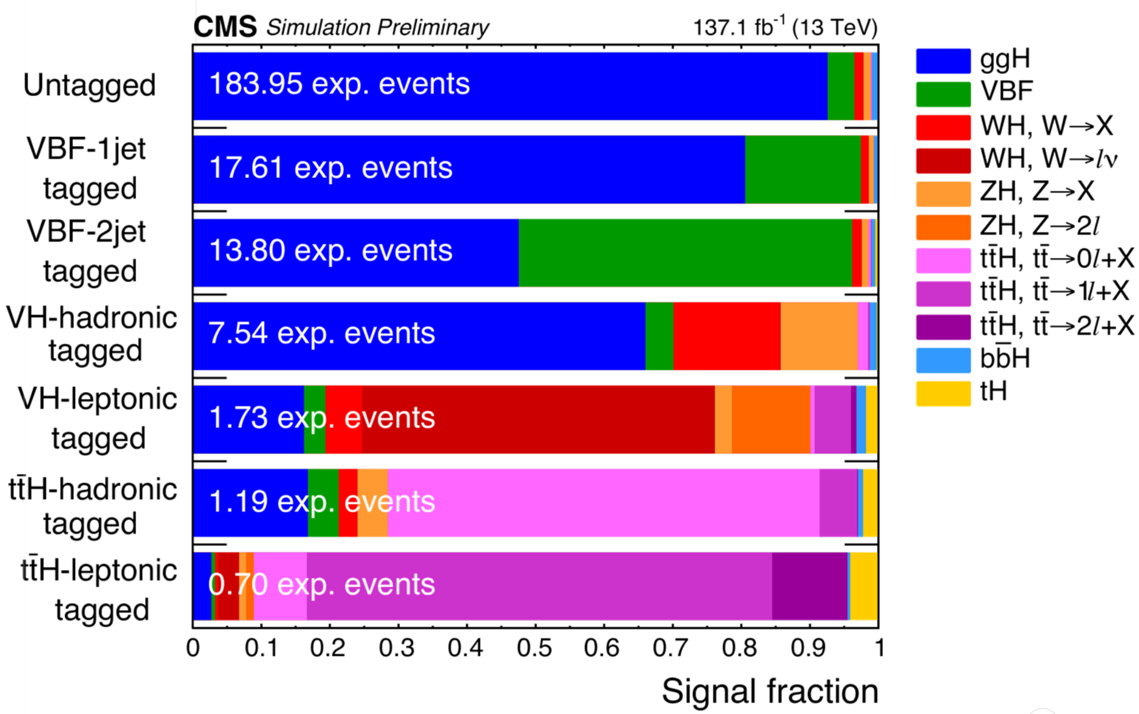

HIG-19-001

CMS $4l$ event yields

Event category	Signal ggH	VBF	WH	ZH	ttH	bbH	tqH	Total signal	Background $q\bar{q} \to ZZ$	$gg \to ZZ$	Z + X	Total expected	Observed
ggH-0j/pT[0,10]	25.3	0.08	0.02	0.02	0.00	0.14	0.00	25.6	26.5	0.97	1.19	54.2	61
ggH-0j/pT[10-200]	86.8	1.69	0.54	0.86	0.00	0.90	0.00	90.8	35.4	3.79	15.5	145	153
ggH-1j/pT[0-60]	26.2	1.43	0.50	0.45	0.01	0.43	0.01	29.1	10.3	1.19	5.54	46.1	40
ggH-1j/pT[60-120]	12.4	1.24	0.45	0.47	0.01	0.10	0.01	14.6	2.76	0.16	3.21	20.8	17
ggH-1j/pT[120-200]	3.31	0.62	0.17	0.26	0.00	0.02	0.00	4.38	0.38	0.00	0.52	5.28	6
ggH-2j/pT[0-60]	3.68	0.29	0.14	0.14	0.06	0.09	0.02	4.42	0.97	0.15	2.07	7.60	9
ggH-2j/pT[60-120]	5.17	0.54	0.22	0.22	0.09	0.04	0.02	6.30	0.84	0.07	1.86	9.06	12
ggH-2j/pT[120-200]	2.90	0.40	0.15	0.17	0.07	0.01	0.02	3.71	0.26	0.00	0.40	4.37	5
ggH/pT>200	2.72	0.65	0.21	0.24	0.06	0.01	0.02	3.91	0.16	0.00	0.21	4.28	2
ggH-2j/mJJ>350	0.82	0.17	0.06	0.05	0.04	0.01	0.01	1.16	0.16	0.02	0.65	1.98	3
VBF-1j	14.2	2.94	0.20	0.18	0.00	0.12	0.01	17.6	2.37	0.43	1.05	21.5	20
VBF-2j/mJJ[350,700]	0.80	1.11	0.01	0.01	0.00	0.01	0.00	1.95	0.08	0.02	0.04	2.09	2
VBF-2j/mJJ>700	0.43	1.80	0.00	0.00	0.00	0.00	0.00	2.25	0.02	0.01	0.03	2.31	2
VBF-3j/mJJ>350	2.43	2.15	0.06	0.07	0.02	0.03	0.05	4.81	0.24	0.06	0.96	6.07	6
VBF-2j/pT>200	0.42	0.76	0.01	0.01	0.01	0.00	0.01	1.22	0.01	0.00	0.03	1.26	0
VBF-rest	2.40	0.87	0.11	0.10	0.03	0.04	0.01	3.56	0.34	0.06	0.74	4.70	2
VH-lep/pTV[0-150]	0.24	0.04	0.71	0.25	0.08	0.02	0.02	1.37	0.82	0.14	0.40	2.72	5
VH-lep/pTV>150	0.02	0.01	0.21	0.08	0.04	0.00	0.01	0.36	0.01	0.00	0.02	0.40	0
VH-had/mJJ[60-120]	4.11	0.25	1.01	1.20	0.11	0.07	0.02	6.77	0.70	0.05	1.36	8.89	8
VH-rest	0.56	0.04	0.08	0.07	0.03	0.00	0.00	0.77	0.08	0.00	0.15	1.01	1
ttH-had	0.19	0.05	0.03	0.06	0.82	0.01	0.03	1.19	0.01	0.00	0.45	1.66	2
ttH-lep	0.02	0.00	0.02	0.02	0.60	0.00	0.03	0.70	0.03	0.00	0.12	0.85	0

Measurements in the $\tau\tau$ channel (ATLAS)

- A test of CP invariance in VBF Higgs boson production was performed in $\tau\tau$ channel with the Optimal Observable method.
- The Optimal Observable (OO) is defined as follows:

$$\mathcal{M} = \mathcal{M}_{\mathrm{SM}} + \tilde{d} \cdot \mathcal{M}_{\text{CP-odd}} \qquad O_{\mathrm{opt}} = \frac{2\,\mathrm{Re}(\mathcal{M}^*_{\mathrm{SM}}\mathcal{M}_{\text{CP-odd}})}{|\mathcal{M}_{\mathrm{SM}}|^2}$$

$$2\,\mathrm{Re}(\mathcal{M}^*_{\mathrm{SM}}\mathcal{M}_{\text{CP-odd}}) = \sum_{i,j,k,l} f_i(x_1) f_j(x_2) 2\,\mathrm{Re}((\mathcal{M}^{ij\to klH}_{\mathrm{SM}})^* \mathcal{M}^{ij\to klH}_{\text{CP-odd}})$$

$$|\mathcal{M}_{\mathrm{SM}}|^2 = \sum_{i,j,k,l} f_i(x_1) f_j(x_2) |\mathcal{M}^{ij\to klH}_{\mathrm{SM}}|^2 .$$

Measurements in the $\tau\tau$ channel (ATLAS)

- A test of CP invariance in VBF Higgs boson production was performed in $\tau\tau$ channel with the Optimal Observable method.
- The Optimal Observable (OO) is defined as follows:

$$\mathcal{M} = \mathcal{M}_{\text{SM}} + \tilde{d} \cdot \mathcal{M}_{\text{CP-odd}} \qquad O_{\text{opt}} = \frac{2\,\text{Re}(\mathcal{M}^*_{\text{SM}}\mathcal{M}_{\text{CP-odd}})}{|\mathcal{M}_{\text{SM}}|^2}$$

$$2\,\text{Re}(\mathcal{M}^*_{\text{SM}}\mathcal{M}_{\text{CP-odd}}) = \sum_{i,j,k,l} f_i(x_1) f_j(x_2) 2\,\text{Re}((\mathcal{M}^{ij\to klH}_{\text{SM}})^* \mathcal{M}^{ij\to klH}_{\text{CP-odd}})$$

$$|\mathcal{M}_{\text{SM}}|^2 = \sum_{i,j,k,l} f_i(x_1) f_j(x_2) |\mathcal{M}^{ij\to klH}_{\text{SM}}|^2 .$$

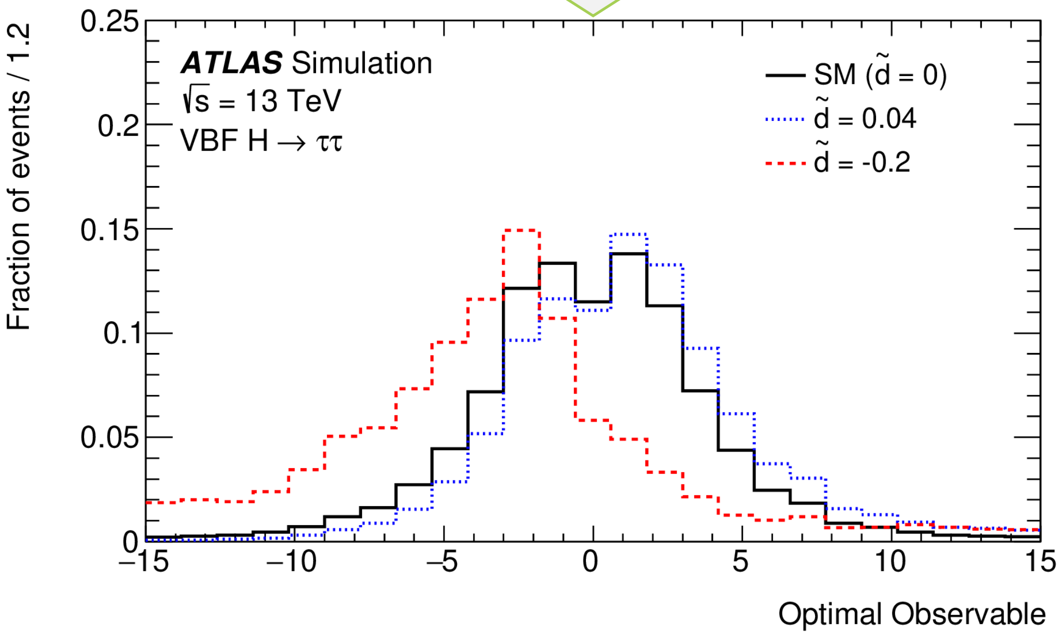

HIGG-2018-14

Measurements in the $\tau\tau$ channel (ATLAS)

- A test of CP invariance in VBF Higgs boson production was performed in $\tau\tau$ channel with the Optimal Observable method.
- The Optimal Observable (OO) is defined as follows:

$$\mathcal{M} = \mathcal{M}_{\rm SM} + \tilde{d} \cdot \mathcal{M}_{\text{CP-odd}} \qquad O_{\rm opt} = \frac{2\,{\rm Re}(\mathcal{M}^*_{\rm SM}\mathcal{M}_{\text{CP-odd}})}{|\mathcal{M}_{\rm SM}|^2}$$

$$2\,{\rm Re}(\mathcal{M}^*_{\rm SM}\mathcal{M}_{\text{CP-odd}}) = \sum_{i,j,k,l} f_i(x_1) f_j(x_2) 2\,{\rm Re}((\mathcal{M}^{ij\to klH}_{\rm SM})^* \mathcal{M}^{ij\to klH}_{\text{CP-odd}})$$

$$|\mathcal{M}_{\rm SM}|^2 = \sum_{i,j,k,l} f_i(x_1) f_j(x_2) |\mathcal{M}^{ij\to klH}_{\rm SM}|^2 .$$

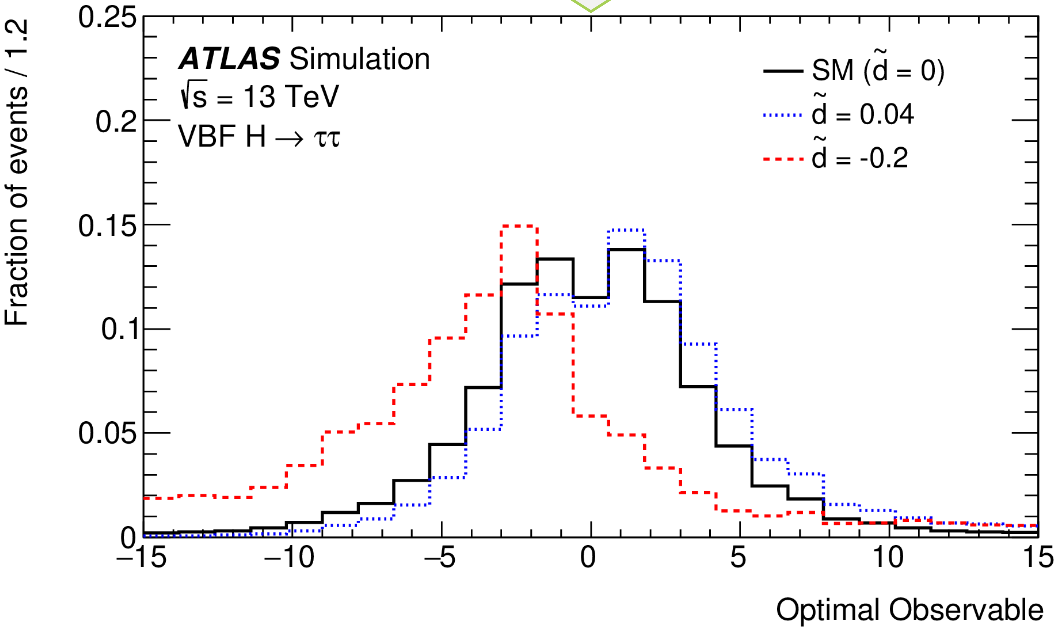

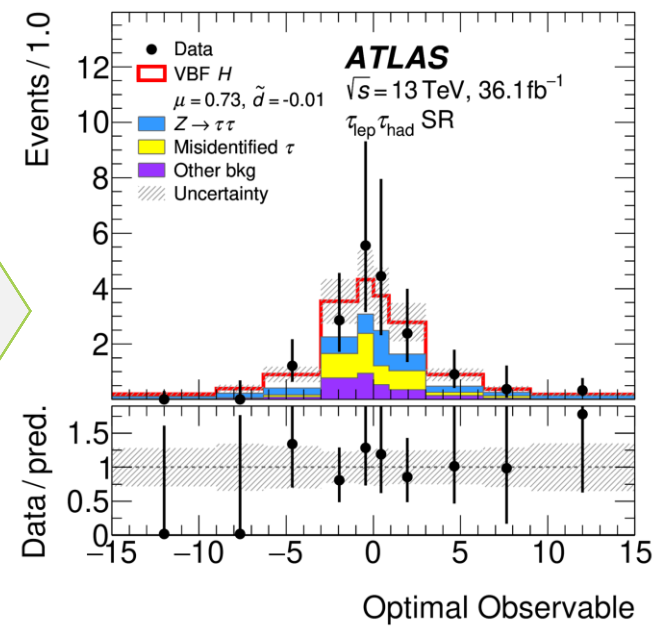

HIGG-2018-14

Measurements in the $\tau\tau$ channel (ATLAS)

- A test of CP invariance in VBF Higgs boson production was performed in $\tau\tau$ channel with the Optimal Observable method.
- The Optimal Observable (OO) is defined as follows:

$$\mathcal{M} = \mathcal{M}_{\mathrm{SM}} + \tilde{d} \cdot \mathcal{M}_{\text{CP-odd}} \qquad O_{\mathrm{opt}} = \frac{2\,\mathrm{Re}(\mathcal{M}^*_{\mathrm{SM}}\mathcal{M}_{\text{CP-odd}})}{|\mathcal{M}_{\mathrm{SM}}|^2}$$

$$2\,\mathrm{Re}(\mathcal{M}^*_{\mathrm{SM}}\mathcal{M}_{\text{CP-odd}}) = \sum_{i,j,k,l} f_i(x_1) f_j(x_2) 2\,\mathrm{Re}((\mathcal{M}^{ij\to klH}_{\mathrm{SM}})^* \mathcal{M}^{ij\to klH}_{\text{CP-odd}})$$

$$|\mathcal{M}_{\mathrm{SM}}|^2 = \sum_{i,j,k,l} f_i(x_1) f_j(x_2) |\mathcal{M}^{ij\to klH}_{\mathrm{SM}}|^2 .$$

Channel	⟨Optimal Observable⟩
$\tau_{\mathrm{lep}}\tau_{\mathrm{lep}}$ SF	-0.54 ± 0.72
$\tau_{\mathrm{lep}}\tau_{\mathrm{lep}}$ DF	0.71 ± 0.81
$\tau_{\mathrm{lep}}\tau_{\mathrm{had}}$	0.74 ± 0.78
$\tau_{\mathrm{had}}\tau_{\mathrm{had}}$	-1.13 ± 0.65
Combined	-0.19 ± 0.37

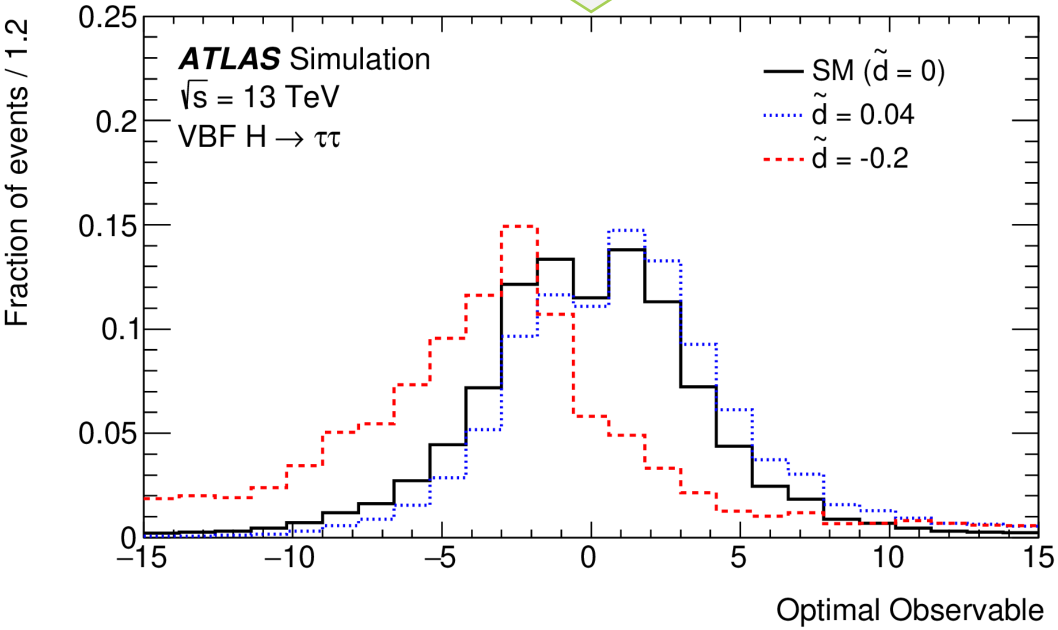

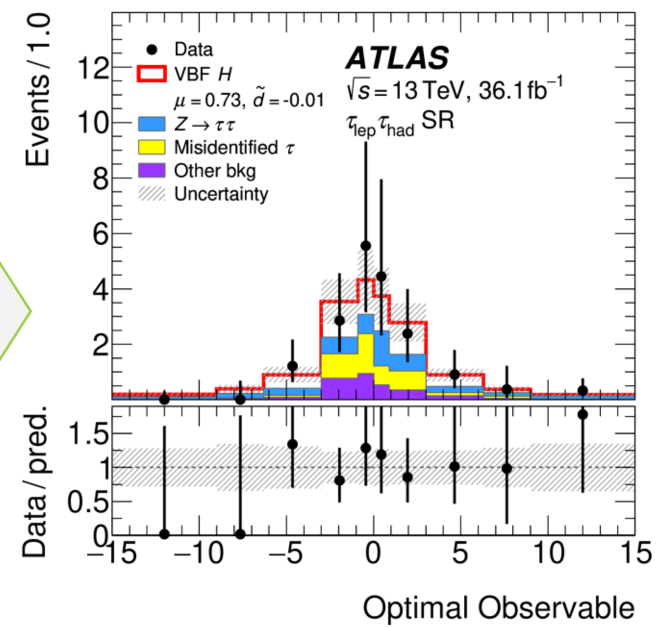

N. Belyaev, 8th annual conference on Large Hadron Collider Physics

HIGG-2018-14

Measurements in the $\tau\tau$ channel (ATLAS)

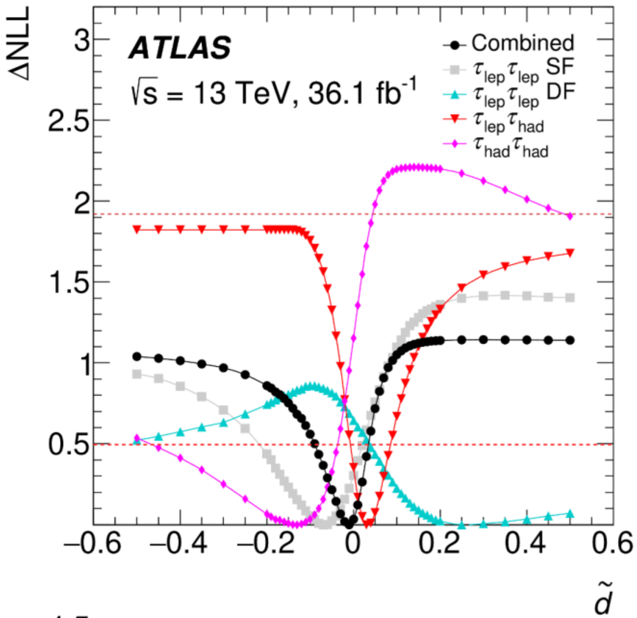

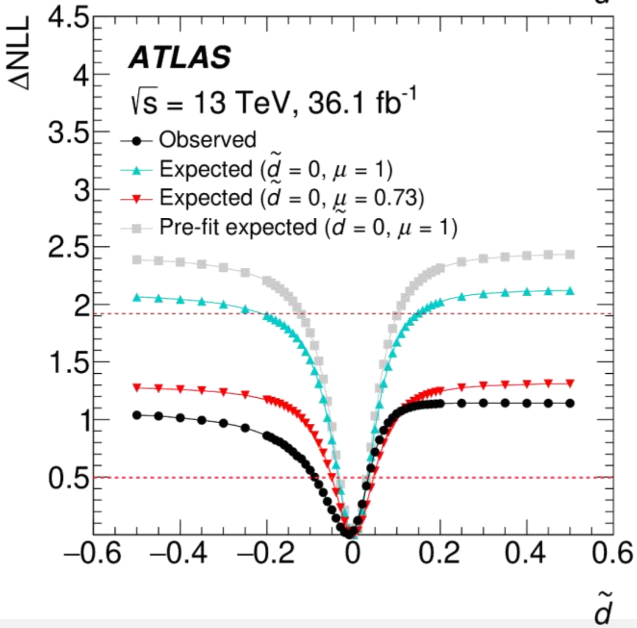

Process	$\tau_{lep}\tau_{lep}$ SF	$\tau_{lep}\tau_{lep}$ DF
Data	26	30
VBF $H \to \tau\tau/WW$ ($\mu = 0.73$, $\tilde{d} = -0.01$)	3.3 ± 2.1	5.1 ± 3.1
VBF $H \to \tau\tau/WW$ ($\mu = 1$, $\tilde{d} = 0$)	4.5 ± 2.9	6.9 ± 4.4
$Z \to \tau\tau$	6.6 ± 3.7	8.2 ± 3.8
Fake lepton	0.02 ± 0.20	2.3 ± 0.7
$t\bar{t}$ + single top	3.8 ± 2.3	10.6 ± 5.5
$Z \to \ell\ell$	11 ± 18	1.8 ± 1.1
Diboson	0.70 ± 0.59	
ggF H / VH / $t\bar{t}H$, $H \to \tau\tau/WW$	0.49 ± 0.48	0.70 ± 0.30
Sum of backgrounds	23 ± 17	23.6 ± 6.1

Process	$\tau_{lep}\tau_{had}$	$\tau_{had}\tau_{had}$
Data	30	37
VBF $H \to \tau\tau$ ($\mu = 0.73$, $\tilde{d} = -0.01$)	11.8 ± 7.4	8.9 ± 5.6
VBF $H \to \tau\tau$ ($\mu = 1$, $\tilde{d} = 0$)	16 ± 10	12.3 ± 7.7
$Z \to \tau\tau$	7.8 ± 3.5	15.5 ± 5.2
Fake lepton/τ	6.2 ± 1.0	5.4 ± 2.7
ggF H / VH / $t\bar{t}H$, $H \to \tau\tau$	2.1 ± 1.5	2.8 ± 1.4
Other backgrounds	2.8 ± 3.1	2.3 ± 0.8
Sum of backgrounds	19.0 ± 5.5	26.0 ± 6.6

- No sign of CP violation is observed in the distributions of the Optimal Observable.

HIGG-2018-14

Measurements in the $\tau\tau$ channel (ATLAS)

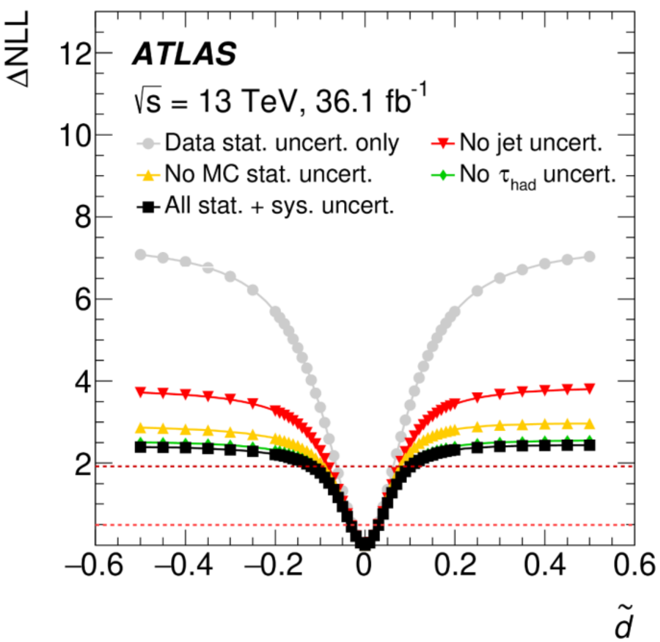

Channel	$\tau_{lep}\tau_{lep}$ SF	$\tau_{lep}\tau_{lep}$ DF	$\tau_{lep}\tau_{had}$	$\tau_{had}\tau_{had}$
Preselection	Two isolated τ-lepton decay candidates with opposite electric charge			
	$p_T^{\tau_1} > 19^*/15^*$ GeV (μ/e) $p_T^{\tau_2} > 10/15^*$ GeV (μ/e)	$p_T^{e} > 18$ GeV $p_T^{\mu} > 14$ GeV	$p_T^{\tau_{had}} > 30$ GeV $p_T^{\tau_{lep}} > 21^*$ GeV $m_T < 70$ GeV	$p_T^{\tau_1} > 40$ GeV $p_T^{\tau_2} > 30$ GeV $0.8 < \Delta R_{\tau\tau} < 2.5$ $\lvert\Delta\eta_{\tau\tau}\rvert < 1.5$ $E_T^{miss} > 20$ GeV
	$m_{\tau\tau}^{coll} > m_Z - 25$ GeV			
	$30 < m_{\ell\ell} < 75$ GeV $E_T^{miss} > 55$ GeV $E_T^{miss, hard} > 55$ GeV	$30 < m_{\ell\ell} < 100$ GeV $E_T^{miss} > 20$ GeV		
	$N_{b\text{-jets}} = 0$			
VBF topology	$N_{jets} \geq 2$, $p_T^{j_2} > 30$ GeV, $m_{jj} > 300$ GeV, $\lvert\Delta\eta_{jj}\rvert > 3$			
	$p_T^{j_1} > 40$ GeV			$p_T^{j_1} > 70$ GeV, $\lvert\eta_{j_1}\rvert < 3.2$
BDT input variables	$m_{\tau\tau}^{MMC}$, m_{jj}, $\Delta R_{\tau\tau}$, $C_{jj}(\tau_1)$, $C_{jj}(\tau_2)$, p_T^{tot}			
	$m_{\tau\tau}^{vis}$, $m_T^{\tau_1, E_T^{miss}}$, $p_T^{j_3}$		$C(\phi^{miss})/\sqrt{2}$	
	$\Delta\phi_{\tau\tau}$	$E_T^{miss}/p_T^{\tau_1}$, $E_T^{miss}/p_T^{\tau_2}$	$m_{\tau\tau}^{vis}$, $\lvert\Delta\eta_{\tau\tau}\rvert$	$p_T^{\tau\tau E_T^{miss}}$, $\lvert\Delta\eta_{\tau\tau}\rvert$
Signal region	$\text{BDT}_{score} > 0.78$		$\text{BDT}_{score} > 0.86$	$\text{BDT}_{score} > 0.87$

Measurements in the $4l$ channel (CMS)

- Properties of the Higgs boson were measured in the $H \to ZZ^* \to 4l\ (l = e, \mu)$ decay channel.
- The STXS measurements were performed for different Higgs boson production channels.

Requirements for the $\mathrm{H} \to 4\ell$ fiducial phase space	
Lepton kinematics and isolation	
Leading lepton p_{T}	$p_{\mathrm{T}} > 20$ GeV
Next-to-leading lepton p_{T}	$p_{\mathrm{T}} > 10$ GeV
Additional electrons (muons) p_{T}	$p_{\mathrm{T}} > 7(5)$ GeV
Pseudorapidity of electrons (muons)	$\lvert\eta\rvert < 2.5(2.4)$
Sum of scalar p_{T} of all stable particles within $\Delta R < 0.3$ from lepton	$< 0.35 \cdot p_{\mathrm{T}}$
Event topology	
Existence of at least two same-flavor OS lepton pairs, where leptons satisfy criteria above	
Inv. mass of the Z_1 candidate	$40\,\mathrm{GeV} < m_{\mathrm{Z}_1} < 120\,\mathrm{GeV}$
Inv. mass of the Z_2 candidate	$12\,\mathrm{GeV} < m_{\mathrm{Z}_2} < 120\,\mathrm{GeV}$
Distance between selected four leptons	$\Delta R(\ell_i, \ell_j) > 0.02$ for any $i \neq j$
Inv. mass of any opposite sign lepton pair	$m_{\ell^+\ell'^-} > 4\,\mathrm{GeV}$
Inv. mass of the selected four leptons	$105\,\mathrm{GeV} < m_{4\ell} < 140\,\mathrm{GeV}$

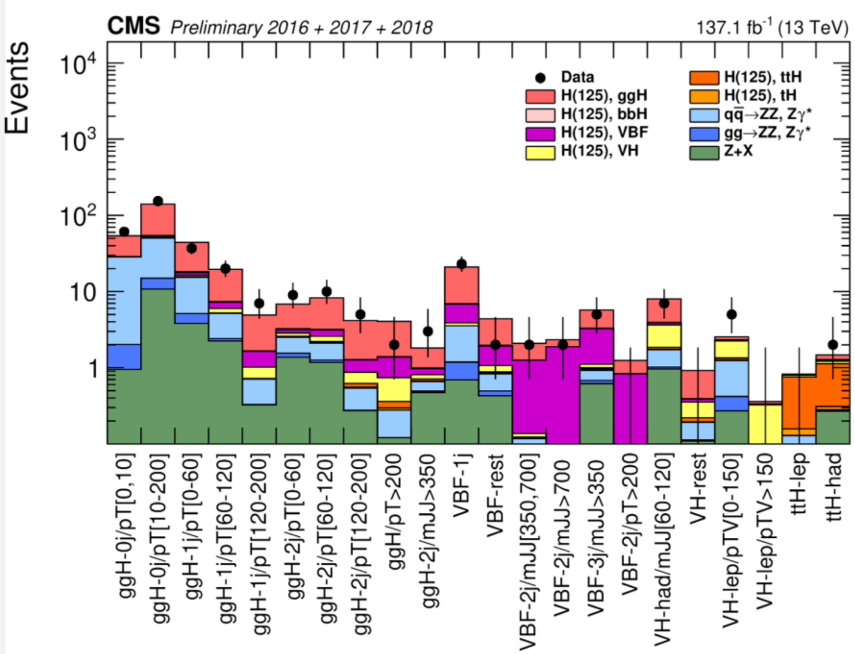

Channel	4e	4μ	$2\mathrm{e}2\mu$	4ℓ
$\mathrm{q\bar{q}} \to \mathrm{ZZ}$	333^{+57}_{-53}	622^{+31}_{-44}	815 ± 73	1770^{+98}_{-101}
$\mathrm{gg} \to \mathrm{ZZ}$	$75.1^{+14.3}_{-13.5}$	$116.6^{+11.7}_{-12.8}$	176.9 ± 23.0	$368.5^{+29.5}_{-29.6}$
Z + X	19.3 ± 7.2	50.8 ± 15.2	64.6 ± 15.6	134.7 ± 22.9
Sum of backgrounds	$428^{+59.2}_{55.2}$	$790^{+36.4}_{-48.3}$	1057 ± 78.1	$2274^{+104.9}_{-107.7}$
Signal ($m_{\mathrm{H}} = 125$ GeV)	$19.6^{+3.3}_{-3.1}$	$40.8^{+2.5}_{-2.9}$	50.7 ± 5.6	$111.1^{+6.9}_{-7.0}$
Total expected	$447^{+59.3}_{55.2}$	$830^{+36.5}_{-48.4}$	1108 ± 78.3	$2385^{+105.1}_{-107.9}$
Observed	462	850	1130	2442

$$
\begin{aligned}
N^{f,i}_{\mathrm{obs}}(m_{4\ell}) &= N^{f,i}_{\mathrm{fid}}(m_{4\ell}) + N^{f,i}_{\mathrm{nonfid}}(m_{4\ell}) + N^{f,i}_{\mathrm{nonres}}(m_{4\ell}) + N^{f,i}_{\mathrm{bkg}}(m_{4\ell}) \\
&= \epsilon^{f}_{i,j} \cdot \left(1 + f^{f,i}_{\mathrm{nonfid}}\right) \cdot \sigma^{f,j}_{\mathrm{fid}} \cdot \mathcal{L} \cdot \mathcal{P}_{\mathrm{res}}(m_{4\ell}) \\
&\quad + N^{f,i}_{\mathrm{nonres}} \cdot \mathcal{P}_{\mathrm{nonres}}(m_{4\ell}) + N^{f,i}_{\mathrm{bkg}} \cdot \mathcal{P}_{\mathrm{bkg}}(m_{4\ell})
\end{aligned}
$$

HIG-19-001

Measurements in the $\tau\tau$ and $4l$ channels (CMS)

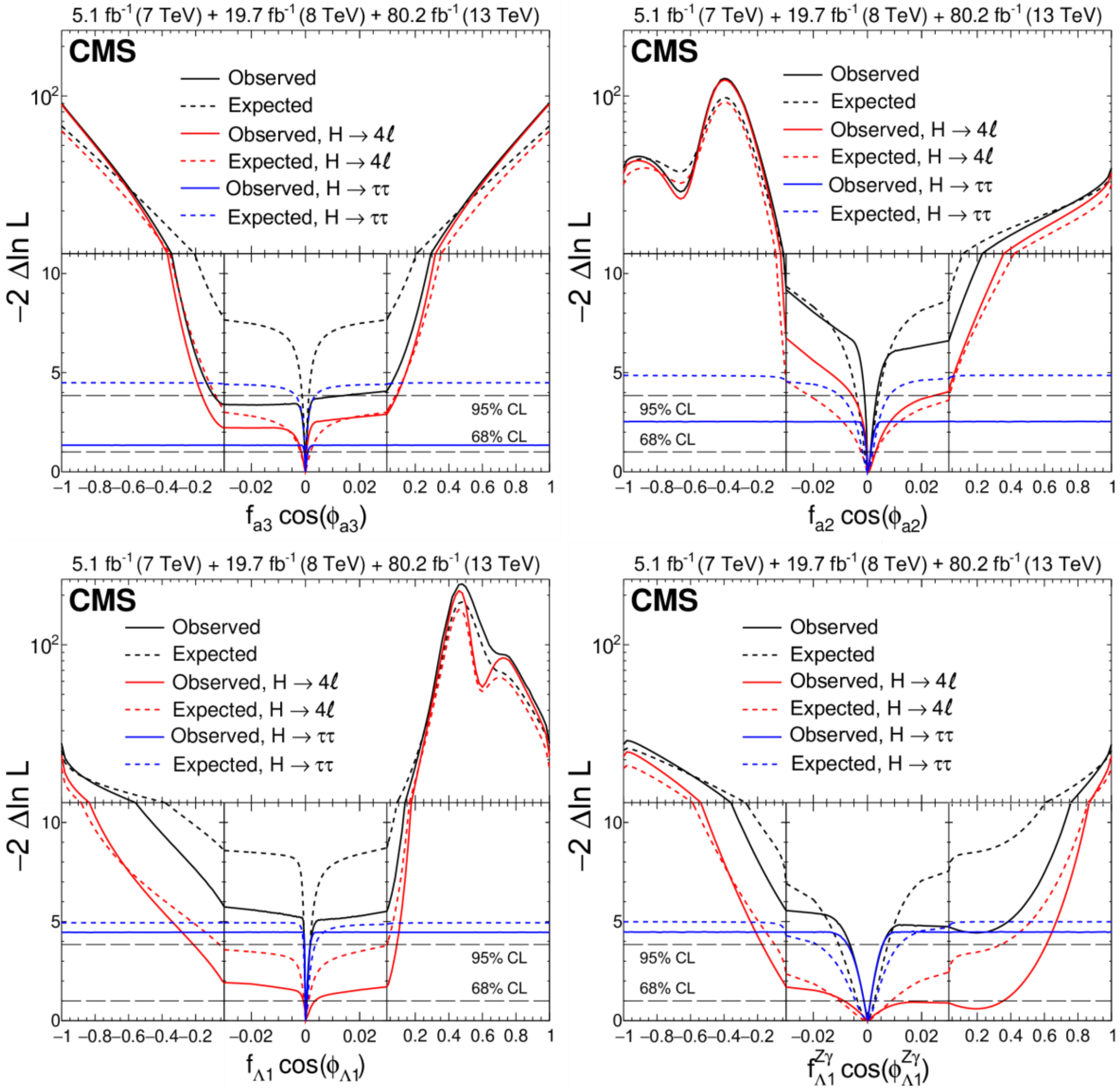

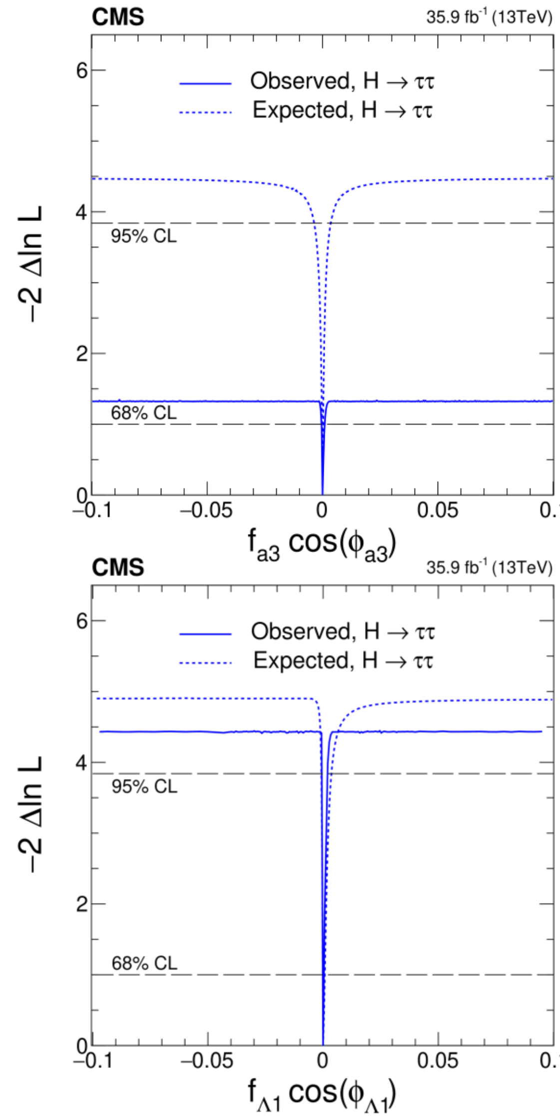

HIG-17-034